Review Article

phys. stat. sol. (b) **175**, 15 (1993)

Subject classification: 72.20 and 72.40; 71.35; 71.38; S12

Fachbereich Physikalische Chemie und Zentrum für Materialwissenschaften der Philipps-Universität, Marburg[1])

Charge Transport in Disordered Organic Photoconductors

A Monte Carlo Simulation Study

By

H. BÄSSLER

Contents

1. Introduction

2. The model

3. Monte Carlo simulation technique

4. Results

4.1 Energetic relaxation
4.2 Dependence of the charge carrier mobility on temperature
4.3 Field dependence of μ and the effect of off-diagonal disorder
4.4 Anomalous broadening of time of flight signals
4.5 Transition from non-dispersive to dispersive transport
4.6 Concentration dependence of μ

5. Guideline for estimating polaronic effects

6. Concluding remarks

References

1. Introduction

To improve the properties of photoconductors requires knowledge concerning the mechanism by which charge carriers are generated and transported. This recognition has recently led to an increased effort, both experimental and theoretical, to clarify the fundamental aspects of charge transport in molecularly doped polymers [1 to 12], main chain [13 to 18], and pendant group polymers [19, 20]. A handicap of earlier work in this field was that photocurrent transients, intended to yield the material property called charge carrier mobility, were notoriously dispersive [21 to 23] indicating that the velocity of a sheet

[1]) Hans-Meerwein-Straße, W-3550 Marburg, FRG.

of carriers started at time $t = 0$ at the front electrode decreased as the packet traversed the sample. Not only is the mean arrival time of carriers at the exit contact of a sandwich sample a poorly defined quantity in that case, it also reflects a system property, i.e. a transport coefficient, that depends on experimental conditions. Meanwhile it has been become clear that a major contribution to the dispersion was the presence of traps of either chemical and physical origin. An example of the latter are incipient dimers in polyvinylcarbazole [24]. It is now well established that non-dispersive photocurrent transients, documented by well developed plateau regions in a time of flight (TOF) experiment, can be observed in appropriately selected and prepared samples. The requirements are (i) high chemical purity, (ii) a molecular structure that does not permit the formation of sandwich-type incipient dimers, and (iii) low ionization potential/large electron affinity to ensure that accidental impurities do not act as traps for holes/electrons. The main intention of this article is to delineate a framework for rationalizing charge transport in polymeric or, more generally, disordered organic photoconductors including the transition from non-dispersive to dispersive transport.

There is a recurrent pattern of features recovered when analysing TOF signals observed with a broad class of molecularly doped polymers like polycarbonate doped with derivatives of triphenylamine [7, 25, 26], hydrazone [5], or pyrazolin [27], to mention only a few, or main chain polymers such as polysilanes [14, 15, 28] or polyphenylenevinylenes [17, 18]. They include (i) an activated behavior of the carrier mobility yielding an activation energy of about 0.4 to 0.6 eV independent of chemical constitution and synthesis if analysed in terms of Arrhenius' equation; (ii) a field dependence of the mobility resembling the Poole-Frenkel law, $\ln \mu \propto SE^{1/2}$, over an extended range of electric fields [4 to 7]; (iii) a deviation of both the magnitude of S and its temperature dependence from the prediction of Poole-Frenkel theory [4, 7]; (iv) a reversal of sign of S above a certain temperature [27], (v) the deviation from a $\ln \mu \propto E^{1/2}$ law at low fields [29] and the occasional occurrence of an increase of μ at decreasing field [17, 30]; (vi) the sensitivity of μ as well as its temperature and field dependence on composition in binary systems [8]; (vii) the existence of tails of TOF signals that are anomalously broad if compared with the tail spreading due to conventional ("thermal") diffusion [31], and (viii) the transition to dispersive transport at low temperatures [20, 23].

The independence of the temperature coefficient of the mobility on chemical composition and the ubiquitous occurrence of a $\ln \mu \propto E^{1/2}$ behavior is clear evidence against the dominance of impurity effects. One can safely exclude that chemically different systems contain (i) the same amount of traps having (ii) the same depth relatively to the transport level and (iii) being charged when empty to account for the $\ln \mu \propto E^{1/2}$ dependence. Instead, one has to conclude that the above features reflect a recurrent intrinsic transport property of the various systems. This, in turn, renders multiple trapping models inadequate for rationalizing charge motion except, e.g., in systems like polyvinylcarbazole known to contain extrinsic traps.

Due to the weak intermolecular coupling valence and conduction bands of molecular crystals are narrow, typically only some 10 meV wide [32]. As a consequence, the mean free path a carrier travels between subsequent phonon scattering events is of order of a lattice distance at room temperature. Given the disorder present in non-crystalline organic solids like molecularly doped polymers which can only shorten the mean free path it is straightforward to assume that the elementary transport step in such systems is the transfer of a charge carrier among adjacent transporting molecules, henceforth called transport sites.

In chemical terms this is a redox process involving chemically identical moieties. The dependence of μ on temperature and electric field must reflect the dependence of that elementary step on T and E. Its activation energy will, in general, be the sum of an intermolecular and an intramolecular contribution. The former arises from the physical inequivalence of the chemically identical hopping sites due to local disorder that subjects the lattice contribution to the energy of a neutral and charged molecule to local, statistical variation [33]. The latter is due to the change in molecular conformation upon removal or addition of an electron from/to the transport molecules (oxidation/reduction). Transfer of a charge, therefore, requires concomitant activated transfer of the deformation [34 to 37]. The essential difference among the currently discussed transport models is related to the relative importance of both contributions. The hopping model assumes that the coupling of the charge to intra(or inter)molecular modes is weak, the activation energy reflecting basically the static energetic disorder of the hopping sites. The (small) polaron model, on the other hand, considers the disorder energy to be unimportant relative to the intramolecular deformation energy.

Unfortunately, there is no direct and easy way to measure the inter- and intramolecular contributions to the transfer activation energy because the optical spectra of molecular solids are controlled by excitonic transitions in contrast to valence band → conduction band transitions in inorganic semiconductors. The density of states (DOS) function for charge transporting states is, thus, not amenable to direct probing by absorption spectroscopy. Quantum chemical calculations, on the other hand, are usually not accurate enough to predict energy differences of the order 0.1 eV. One has, therefore, to rely on the analogy of the coupling between an exciton and a charge carrier, on the one hand, and the surrounding lattice, on the other hand, in order to estimate the width of the disorder-broadened DOS. Consider both a charge carrier and an excited state dipole surrounded by a polarizable medium. To first order approximation their polarization energy P_c and gas to solid shift energy D are determined by ion–dipole and dipole–dipole coupling, obeying r^{-4} and r^{-6} dependences on intersite distances, respectively. Absolute values are typically $P_c \approx 1.2$ eV [38] and $D \approx 0.25$ eV, respectively, and exceed the intermolecular exchange energies by almost two orders of magnitude [32]. In random media intermolecular distances and, concomitantly, P_c and D fluctuate, their relative

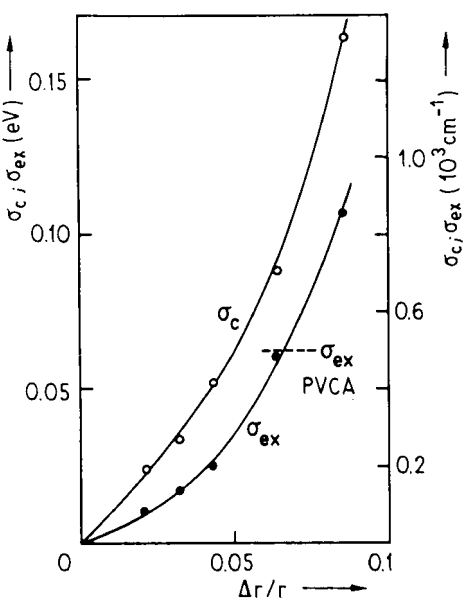

Fig. 1. Standard deviations of the widths of the DOS for charge carriers (σ_c) and excitations (σ_{ex}) calculated for $P_c = 1.2$ eV and $D = 0.25$ eV. The width of the DOS for the $S_1 \leftarrow S_0$ 0–0 transition in polyvinylcarbazole is indicated (from [39])

standard deviations being [39]

$$\sigma_c/P_c = \sum_{i \neq j} (\Delta r_{ij}/r_{ij})^4$$

and

$$\sigma_{ex}/D = \sum_{i \neq j} (\Delta r_{ij}/r_{ij})^6 ,$$

respectively. The data shown in Fig. 1 were obtained by doing summation and averaging on a computer system consisting of a cubic array of 300 point sites each being allowed to fluctuate about its mean crystallographic position. They demonstrate that the width of the DOS for charge carriers originating from a given pattern of positional disorder is about 1.5 times as big as that for singlet excitation. Measuring the DOS for singlet excitations thus permits concluding on the width of the DOS for charge carriers as well.

Absorption (and fluorescence) bands of disordered organic solids are usually of Gaussian shape with a standard deviation (Gaussian width) of typically $\sigma_{ex} = 500\,\text{cm}^{-1}$ (60 meV) [40]. On the basis of the above argument one expects that the inhomogeneously broadened DOS for charge carriers are also of Gaussian shape, the Gaussian width σ being of order 0.1 eV translating into an activation energy of about 0.4 eV (see Section 4.1). Site-selective fluorescence spectroscopy of the pertinent transport materials, on the other hand, yields a fluorescence Stokes shift that is one order of magnitude less [41]. This can be considered as a justification for starting with a hopping model as a zero-order approach that does not include polaronic effects, in particular since an analysis of charge motion in a prototypical molecular crystal (naphthalene) suggested a polaronic binding energy of 16 meV only [42].

2. The Model

To model hopping transport across a disordered single or multiple component organic solid the charge transporting elements, which can either be the molecules participating in transport or segments of a main chain polymer that are separated by topological defects, are identified as sites whose energies of their hole or electron transporting states are subject to a Gaussian distribution of energies,

$$\varrho(\varepsilon) = (2\pi\sigma^2)^{-1/2} \exp\left(-\frac{\varepsilon^2}{2\sigma^2}\right), \tag{1}$$

implying that all states are localized. The energy ε is measured relative to the center of the DOS. The origin of the energetic (diagonal) disorder is the fluctuation of the lattice polarization energies and/or the distribution of segment length in π- or σ-bonded main chain polymer. The Gaussian shape of the DOS is suggested by the Gaussian profile of the (excitonic) absorption band and by the recognition that the polarization energy is determined by a large number of internal coordinates each varying randomly by small amounts [33]. The tacit assumption contained in (1) is that the self-energies of adjacent sites are uncorrelated. This may not strictly be true, yet since structural correlation lengths in organic glasses do not exceed a few intermolecular distances at most, it appears to be a reasonable premise, in particular since a carrier visits typically some 10^4 to 10^5 sites on its way across either a simulation or a real world sample.

The jump rate among sites i and j is assumed to be of the Miller-Abrahams type, i.e. is the product of a prefactor ν_0, an electronic wave function overlap factor, and a Boltzmann factor for jumps upward in energy [43],

$$\nu_{ij} = \nu_0 \exp\left(-2\gamma a \frac{\Delta R_{ij}}{a}\right) \begin{cases} \exp -\dfrac{\varepsilon_j - \varepsilon_i}{kT}; & \varepsilon_j > \varepsilon_i, \\ 1; & \varepsilon_j < \varepsilon_i. \end{cases} \tag{2}$$

In (2) a is the average lattice distance. In case of an applied electric field E the site energies include the electrostatic energy term. Equation (2) implies that the electron–phonon coupling is weak enough to render polaronic effects negligible, yet sufficiently strong to guarantee coupling to the heat bath. Notice that there is no other activation energy except the difference in electronic site energies a carrier has to overcome in order to hop. Hops down in energy are not impeded by an energy matching condition for dissipation of the electronic energy difference. Considering the rich phonon spectra and the low charge exchange rates compared to typical phonon frequencies this appears to be an uncritical assumption. The above form of the jump rate also implies that downward jumps are not accelerated by an electric field.

To consider that (i) in a disordered medium the intersite distance is subject to local variation and, more importantly, (ii) coupling among the transport molecules, which are usually non-spherical, depends on mutual orientation [37] and is, therefore, also disorder affected, the overlap parameter $2\gamma a = \Gamma$ is subjected to distribution as well (off-diagonal disorder). Operationally this is done by splitting the intersite coupling parameter Γ_{ij} into two site specific contributions Γ_i and Γ_j, each taken from a Gaussian probability density of variance σ_Γ. The variance of Γ_{ij} is $\Sigma = 2\sqrt{\sigma_\Gamma}$. This is an arguable procedure. It implies some correlation because all jumps from a given site are affected by the choice of Γ_i. Choosing a Gaussian for the probability density of Γ_{ij} appears to be even more critical since, as Slowik and Chen [44] have shown, the overlap parameter is a complicated and strong function of the mutual molecular angles. In the absence of any explicit knowledge about the actual distribution of overlap parameters a Gaussian appears to be a zero-order choice, in particular since the relative fluctuation $\Sigma/2\gamma a$ required to fit experimental data turns out to hardly exceed ≈ 0.3. In any event, Σ should be considered as an operationally defined measure of the off-diagonal disorder that cannot be directly translated into a microscopic structural picture in contrast to the parameter characterizing diagonal disorder.

3. Monte Carlo Simulation Technique

Unfortunately, the Gaussian form of the DOS in random organic systems prevents closed form analytical solutions of the hopping transport problem. The only analytical theory available to date that retains both the energetic distribution of hopping sites and the distribution of hopping barriers is the effective medium approach (EMA) developed by Movaghar and coworkers [45]. The higher-order correlation effects appearing when summing over all paths a particle can take on going from site i to j lead in this approximation to an effective reduction of the site density after each jump. It has been shown that for finite temperatures the EMA provides an excellent description of the hopping process in dense systems [46], its disadvantage being that it does not provide the experimentalist with analytic equations ready to fit experimental data. The EMA is superior to the *ultrametric space*

concept [47 to 49] which is mathematically simpler and avoids the averaging technique involved in the effective medium treatment but does so at the expense of reducing the real energy structure of the system to an array of isoenergetic hopping sites separated by randomly distributed barriers.

The alternative approach this article elaborates on is Monte Carlo (MC) simulation [50]. It can be considered as an idealized experiment carried out on samples of arbitrarily adjustable degree of disorder and devoid of any accidental complexity. It allows to determine which level of sophistication is required to reproduce the properties of a real world sample and, by comparison with theory, to check the validity of approximations in analytical treatments that are based on the same physical principles.

The current MC simulations were performed on a cubic lattice consisting of $70 \times 70 \times 70$ sites with site distance $a = 0.6$ nm. Their self-energies and Γ_i-values were chosen according to a Gaussian probability density. By applying periodic boundary condition an effective sample size of up to $8000 \times \infty \times \infty$, equivalent to a sample length of 4.8 μm in x-direction, which is the direction of an applied electric field, was considered. Usually 20 carriers are started one at a time on an arbitrary site of a given lattice configuration. Afterwards a new lattice is set up. The total number of carriers considered for a TOF pulse is 100 to 150. This turned out to be a reasonable compromise between computer time and computational statistics.

The probability that a carrier jumps from a site i to any site j within a cube consisting of $7 \times 7 \times 7$ sites is

$$P_{ij} = \nu_{ij} / \sum_{i \neq j} \nu_{ij} . \tag{3}$$

A random number x_R from a uniform distribution is chosen and this specifies to which site the particle jumps because each site is given a length in random number space according to P_{ij}. The time for the jump is determined from

$$t_{ij} = x_{ci} \left(\sum_{l \neq i} \nu_{il} \right)^{-1} , \tag{4}$$

where x_{ci} is taken from another exponential distribution of random numbers. The time scale is defined by the dwell time

$$t_0 = (6\nu_0 \exp(-2\gamma a))^{-1} \tag{5}$$

of a carrier on a site in a lattice without disorder. The computational variables are (i) the reduced energetic disorder parameter $\hat{\sigma} = \sigma/kT$, (ii) Σ at constant $2\gamma a = 10$, and (iii) the applied electric field. The computer kept track of the mean position $\langle x \rangle$ and the time-weighted mean energy $\langle \varepsilon \rangle$ of a carrier as well as the related variances as a function of time. The carrier mobility is inferred from the mean carrier arrival time at the exit contact. Its determination from the current plateau in a non-dispersive TOF signal yields identical results. The apparent diffusivity is calculated from the spatial variance of the carrier packet,

$$D = \langle (x - \langle x \rangle)^2 \rangle / 2t . \tag{6}$$

Keeping track of the evolution of $\langle (x - \langle x \rangle)^2 \rangle$ as the packet moves across the sample allows concluding on the spreading of the TOF signal in systems of arbitrary length up to 8000 lattice planes.

4. Results

4.1 Energetic relaxation

A particle started at arbitrary energy within a Gaussian DOS of an undiluted system of hopping sites is likely to execute a random walk and relax into tail states. It is a specific feature of a Gaussian as compared with an exponential DOS that the mean energy, $\langle\varepsilon\rangle$, saturates at long times indicating attainment of dynamic equilibrium. Notice that true thermodynamic equilibrium will never be established since the hopping motion of an excess carrier, generated externally by photoexcitation or injection, is considered. Contrary to the case of hopping at the Fermi level of amorphous inorganic semiconductors [51], Fermi statistics is irrelevant since the carrier is considered to move in an otherwise empty DOS. This corresponds to charge carrier densities that are low enough to exclude carrier–carrier interaction in real experiment. The equilibration energy $\langle\varepsilon_\infty\rangle$ of a carrier at zero electric field can be calculated analytically from [46]

$$\langle\varepsilon_\infty\rangle = \lim_{t\to\infty}\langle\varepsilon(t)\rangle = \frac{\int_{-\infty}^{+\infty}\varepsilon\varrho(\varepsilon)\exp(-\varepsilon/kT)\,\mathrm{d}\varepsilon}{\int_{-\infty}^{+\infty}\varrho(\varepsilon)\exp(-\varepsilon/kT)\,\mathrm{d}\varepsilon} = -\frac{\sigma^2}{kT} = -\sigma\hat{\sigma}\,. \tag{7}$$

Note that $\langle\varepsilon_\infty\rangle$ is independent of the presence of off-diagonal disorder. Fig. 2 portrays the temporal evolution of a packet of non-interacting carriers relaxing within a Gaussian DOS. As time progresses the shape of the packet becomes slightly asymmetric, the high-energy wing of the occupational DOS ($\mathrm{DOS}^{\mathrm{occ}}$) equilibrating earlier. In the long-time limit $\langle\varepsilon_\infty\rangle = -\sigma\hat{\sigma}$ and the shape of the $\mathrm{DOS}^{\mathrm{occ}}$ becomes Gaussian and acquires a width σ indicating that dynamic equilibrium has been established. The temporal variation of $\langle\varepsilon\rangle$, parametric in $\hat{\sigma}$, is shown in Fig. 3. It demonstrates that $\langle\varepsilon(t)\rangle$ relaxes approximately yet

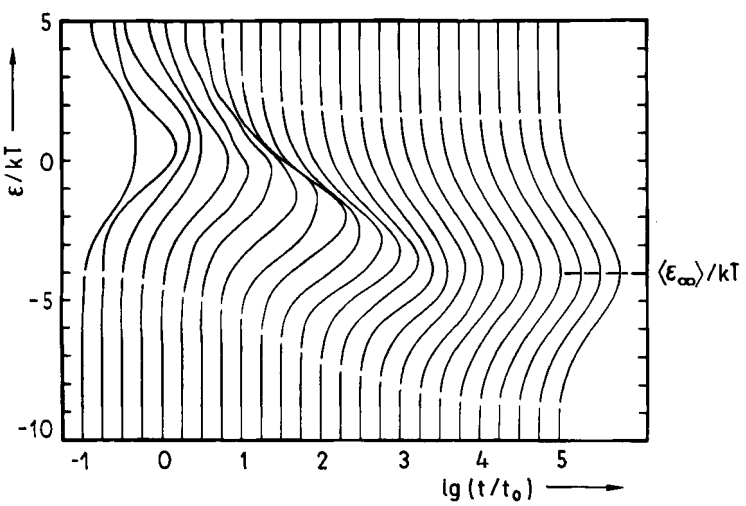

Fig. 2. Temporal evolution of the distribution of carrier energies in a Gaussian DOS of width $\hat{\sigma} = 2$. All profiles are broken at the same carrier density illustrating the different relaxation patterns for mobile and immobile carriers. ε_∞ denotes the theoretical mean energy in the long-time limit

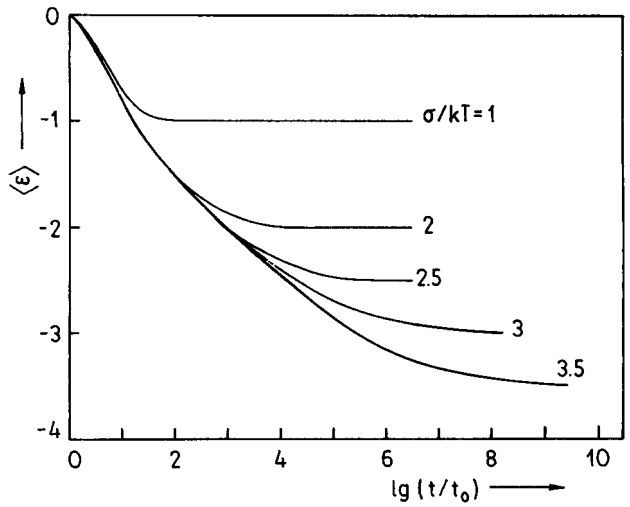

Fig. 3. Temporal decay of the mean energy of an ensemble of carriers migrating within a Gaussian DOS of variable normalized width $\hat{\sigma}$

not strictly logarithmically with time, in quantitative agreement with analytic EMA results [46]. The relaxation time obeys the empirical relationship [52]

$$t_{rel}/t_0 = 10 \exp\left(-(1.07\hat{\sigma})^2\right). \tag{8}$$

In the $T \to 0$ limit relaxation is slowed down since intervening thermally activated jumps that help a carrier finding additional pathways for relaxation are eliminated [53].

There is no direct probe for the relaxation of charge carriers in organic media. However, triplet excitation can serve as probe particles, albeit with finite lifetime, since they are transported via exchange interactions as charge carriers are. It was gratifying to note that the relaxation of triplet excitation in a benzophenone glass occurs in quantitative agreement with both simulation and analytic theory [54, 55]. This testifies on the adequacy of the basic assumptions underlying the model, in particular, the form of the jump rate (2).

4.2 Dependence of the charge carrier mobility on temperature

For $\hat{\sigma} = 4$, i.e. $\sigma \approx 0.1$ eV at 295 K, which turns out to be a representative value of the energetic disorder parameter for many experimental systems, $\langle \varepsilon_\infty \rangle = -4\sigma$. Since the fractional DOS for $\varepsilon \leqq \langle \varepsilon_\infty \rangle$ is $\int_{-\infty}^{-4\sigma} g(\varepsilon)\, d\varepsilon \approx 3 \times 10^{-5}$ only, a carrier located at $\varepsilon = \langle \varepsilon_\infty \rangle$ can, on average, continue its motion only after thermal excitations. If all carriers were exactly located at $\varepsilon = \langle \varepsilon_\infty \rangle = \hat{\sigma}\sigma$ and if a transport level existed exactly at the center of the DOS ($\varepsilon = 0$) the transport activation energy were $\hat{\sigma}\sigma$, i.e. $\mu(T)$ should follow a non-Arrhenius-type temperature dependence, $\mu(T) = \mu_0 \exp\left(-(\sigma/kT)^2\right)$. Both EMA and MC studies indicate that this characteristic temperature dependence, that has been derived in other context, too [56 to 58],[2]) is actually recovered, albeit with a prefactor less than unity in the exponent that accounts for the statistics of both the occupational energies and

[2]) The first report suggesting this form of temperature dependence of a transport coefficient in a random system appears to be the work of Ferry et al. [59] on the temperature dependence of the viscosity in poly(isobutylene) above the glass transition temperature.

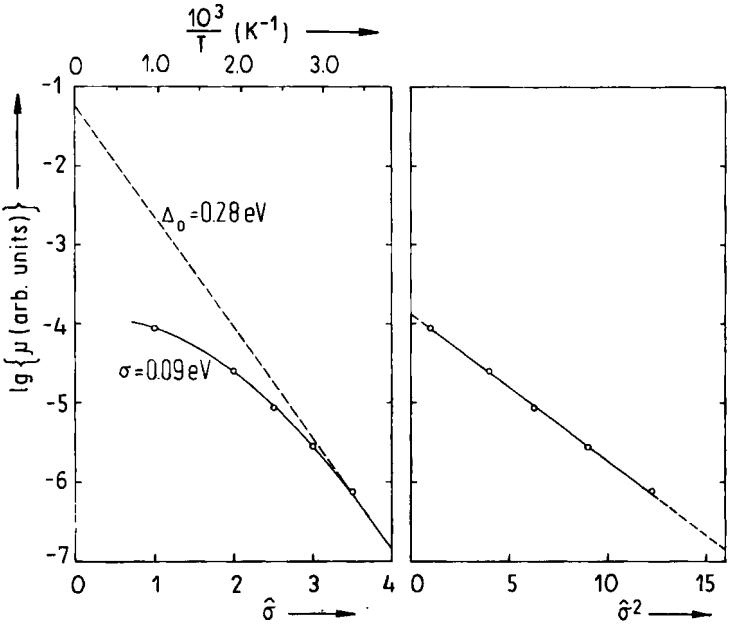

Fig. 4. Simulation result for the dependence of the low-field charge carrier mobility on the degree of energetic disorder ($\hat{\sigma} = \sigma/kT$) plotted on $\ln \mu$ vs. $\hat{\sigma}$ and $\hat{\sigma}^2$ scales, respectively. (In the computations σ was varied.) An Arrhenius fit chosen to match the data in the vicinity of 300 K is included for comparison

the barrier heights,

$$\mu(T) = \mu_0 \exp\left(-(\tfrac{2}{3}\hat{\sigma})^2\right). \tag{9}$$

The prefactor in the exponent is associated with an incertainty of 4%. Fig. 4 shows $\mu(T)$ plotted semilogarithmically versus T^{-1} (Fig. 4a) and T^{-2} (Fig. 4b). The latter representation provides the better fit although it is also obvious that the distinction becomes the more difficult the smaller the range of $\hat{\sigma}$ or temperature is. By differentiation one can infer from (9) the Arrhenius activation energy obtained if one plotted $\mu(T)$ in an Arrhenius fashion and determined the apparent activation energy Δ_0 from the slope at a given temperature T,

$$\Delta_0 = -k \frac{\partial \ln \mu}{\partial (1/T)} = \frac{8}{9} \hat{\sigma}\sigma. \tag{10}$$

An apparent activation energy of 0.4 eV, inferred from the tangent to an Arrhenius plot at 300 K would thus be expected for a hopping system characterized by a DOS of width $\sigma \approx 0.108$ eV as expected on the basis of the width of optical absorption bands (Section 1). An experimental example for the T-dependence of the hole mobility in an organic glass – a vapor-deposited film of 1,1-bis(di-4-tolylaminophenyl)cyclohexane (TAPC) – is presented in Fig. 5 (from [60]). Although the deviations are small the $\ln \mu$ versus T^{-2} fit is clearly the better fit. Another example is contained in the early work of Schein et al. on hole transport in p-diethylaminobenzaldehyde-diphenylhydrazone (DEH) doped into a polycarbonate matrix [5]. Although this was the first demonstration of the superiority of the

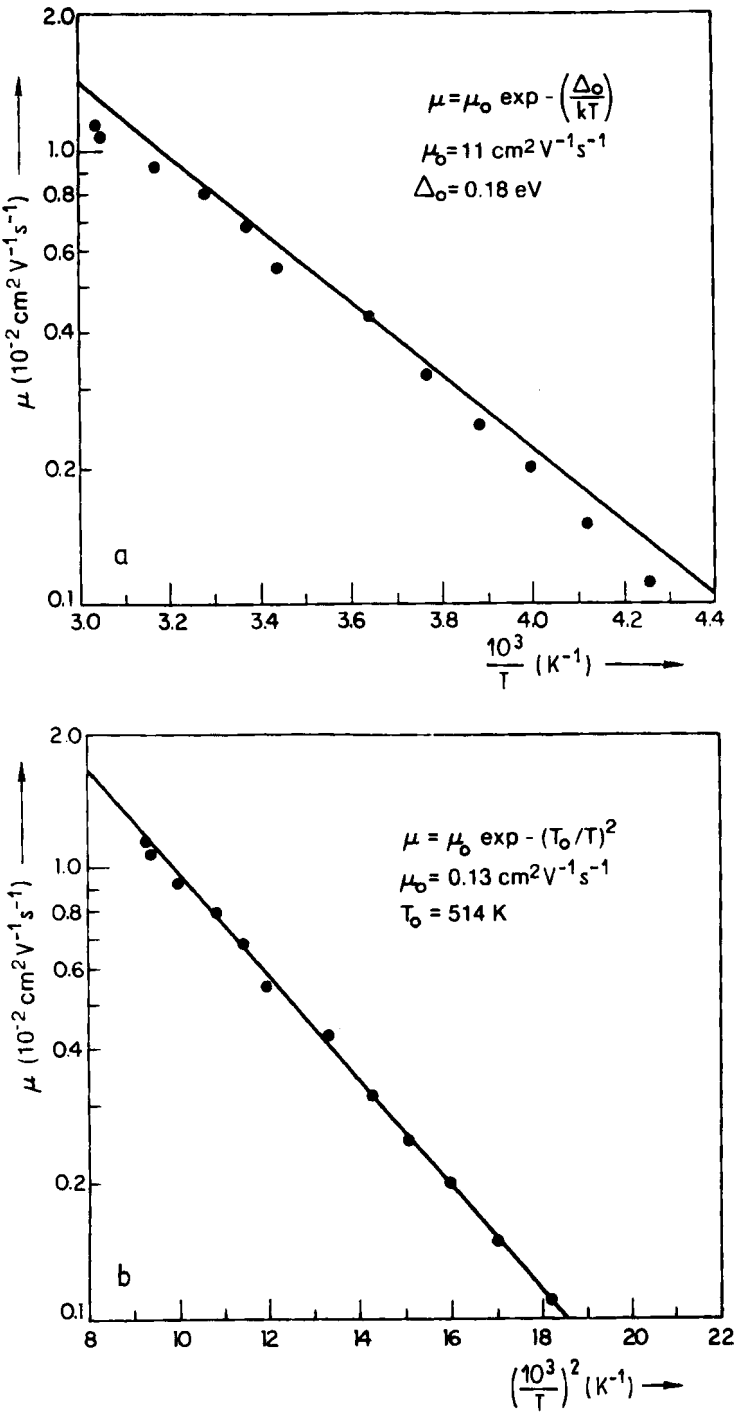

Fig. 5. Temperature dependence of the hole mobility in amorphous TAPC in ln μ vs. a) T^{-1} and b) T^{-2} representation, respectively (from [60])

ln μ versus T^{-2} representation of $\mu(T)$ data for organic glasses these authors revised their interpretation later on [6, 26] in favor of the conventional Arrhenius analysis in order to promote the polaron concept.

An argument in favor of the application of (9) to analyse experimental $\mu(T)$ data comes from the μ_0 data obtained by extrapolation to $T \to \infty$. While the Arrhenius plot notoriously overestimates μ_0 – values are typically $\approx 10\,\mathrm{cm^2\,V^{-1}\,s^{-1}}$ or larger which is unrealistical for a non-crystalline and usually diluted molecular solid – (9) yields values of order 10^{-2} to $10^{-1}\,\mathrm{cm^2\,V^{-1}\,s^{-1}}$ as expected. The comparison between experimental μ_0-values and the mobility in a molecular solid should, however, be considered with some caution because, on the one hand, the latter is expected to exceed those in an energetically ordered hopping system because of coherence effects and, on the other hand, the former may be enhanced by off-diagonal disorder (see below).

4.3 Field dependence of μ and the effect of off-diagonal disorder

The hopping mobility must depend on an applied electric field E since tilting the DOS by an electrostatic potential reduces the average barrier height for energetic uphill jumps in field direction. As a consequence the equilibration energy $\langle \varepsilon_\infty \rangle$ must increase with E. Heating the carrier gas at high electric fields is a common effect in semiconductors and is usually related to the k-dependence of the electron–phonon coupling. In the present model it is solely a consequence of the effect the field has on the interplay between upward and downward jumps of a carrier anticipating that the coupling to the heat bath remains unaffected. Fig. 6 shows that $\langle \varepsilon_\infty \rangle$ increases with E according to

$$\langle \varepsilon_\infty \rangle = \hat{\sigma}\sigma + (E/E_0)^{1.5} \tag{11}$$

with $E_0 = 1.8 \times 10^6\,\mathrm{V\,cm^{-1}}$ being independent of $\hat{\sigma}$. For $\hat{\sigma} = 2$ saturation occurs above $2 \times 10^6\,\mathrm{V\,cm^{-1}}$. The deviation of the data points for $\hat{\sigma} = 3.5$ and fields below $1.5 \times 10^6\,\mathrm{V\,cm^{-1}}$ reflects the fact that at this degree of disorder equilibrium is not fully reached in the

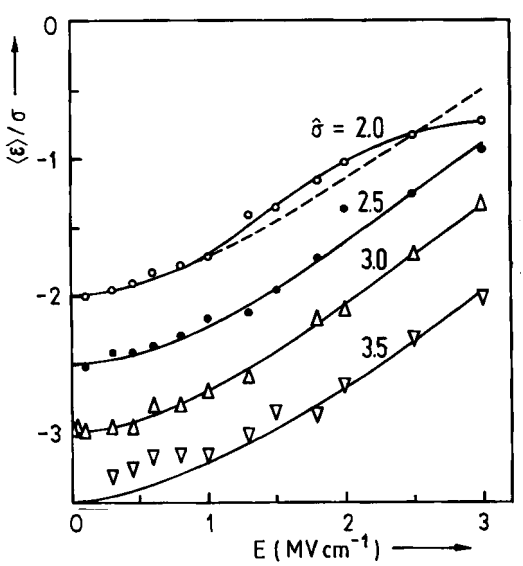

Fig. 6. MC result for $\langle \varepsilon \rangle / \sigma$ as a function of the electric field, parametric in $\hat{\sigma}$

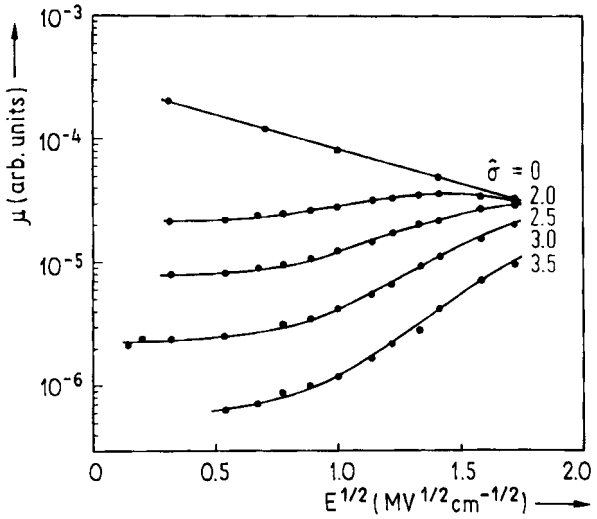

Fig. 7. Simulated dependence of μ on $E^{1/2}$, for variable $\hat{\sigma}$

simulation even with a sample consisting of 8000 lattice planes. The concomitant variation of μ with E is portrayed in Fig. 7 for a hopping system subject to energetic disorder only. The S-shaped $\langle \varepsilon_\infty \rangle$ versus E relationship is retained in the $\ln \mu$ versus $E^{1/2}$ plot [61]. $\mu(E)$ saturates at low fields and increases in a Poole-Frenkel fashion at higher fields. The deviations from a $\ln \mu \propto E$ law are small, however. It was for this reason why it has not been recovered in earlier MC work [62], done on smaller samples. At vanishing disorder, μ decreases with E at large fields. This simply reflects the saturation of the drift velocity with field in a hopping system with isoenergetic sites in which the field does not affect intersite jump rates. The data of Fig. 7 demonstrate that the assumption of a hopping system with Gaussian DOS is sufficient to reproduce $\ln \mu = SE^{1/2}$ behavior within a limited field interval, the slope parameter S changing sign below a certain value of $\hat{\sigma}$, i.e. above a certain temperature. Meanwhile Movaghar et al. [63] have developed an analytic theory for the $\mu(E)$ behavior. They found that a $\ln \mu \propto E^n$ law with $0 < n < 0.5$ is a characteristic feature of hopping motion, the value of the exponent being determined by the shape of the DOS.

An experimental system revealing saturation of μ at low fields and $\ln \mu \propto E^{1/2}$ behavior at higher fields is poly(methylphenylsilane) (PMPS) [29] (Fig. 8). It is, however, obvious that the $\ln \mu \propto E^{1/2}$ law is valid down to lower fields than found by simulation. Part of this discrepancy is due to the definition of the transit time. In simulation, μ is calculated from the mean arrival time of the carriers while in experiment it is inferred from either the time t_0 at which the tangents to plateau and tail intersect or the time $t_{1/2}$ after which the current has decayed to 1/2 of its plateau value.[3]) Simulated TOF signals (see Section 4.4, Fig. 16) indicate, however, that the true transit time rather corresponds to the time at which the current has decayed to $\approx 1/4$ of its plateau value [64] (for further discussion see Section 4.4). While being of little importance for absolute mobility measurements, the different definitions are important as far as the field dependence of μ is concerned because of the field dependence of the dispersion of the tails of what are normally referred to as non-dispersive

[3]) *Note added in proof:* Meanwhile a more accurate way of determining charge carrier mobilities from experimental TOF signals has been proposed [98]. It yields μ-values in accord with the definition used in the simulation.

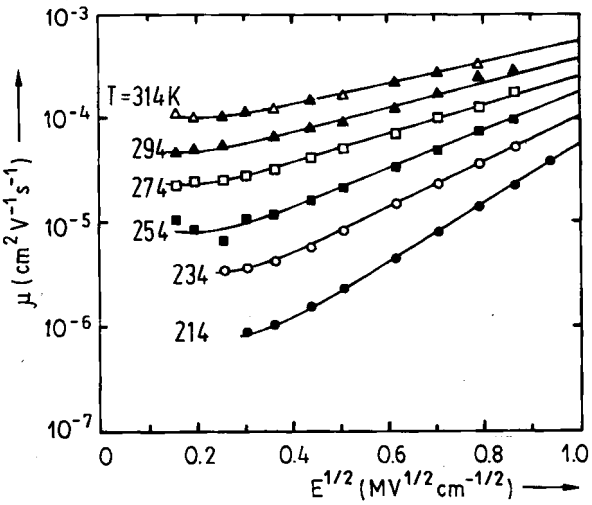

Fig. 8. Logarithm of μ against $E^{1/2}$ for PMPS films at various temperatures: ● 214 K, ○ 234 K, ■ 254 K, □ 274 K, ▲ 294K, △ 314 K (from [29])

TOF signals. Fig. 9 illustrates that inferring μ from t_0 extends the field range of the validity of the $\ln \mu \propto E^{1/2}$ by a factor of 3 towards lower fields. Further, since the essential quantity determining the $\mu(E)$ relation is the drop of the electrostatic potential across an intersite distance, normalized to kT, the simulation field has to be rescaled by the factor 0.6 nm/a^{exp}, a^{exp} being the experimental mean intersite distance, for comparing experimental with MC data. A cautionary note is also in order regarding the reliability of low-field mobility data. The larger the transit time is the more likely becomes capture by a low concentration of deep traps. This would lower the effective mobility. Delayed injection from an injection layer or delayed geminate pair dissociation in the bulk may be another spurious effect tending to bend down the $\mu(E)$ curves at low fields.

Before embarking on a discussion of the T-dependence of the slope parameter S, the effect of off-diagonal disorder on the $\mu(E)$-relation shall be addressed. Superimposing variable off-diagonal disorder, quantified by the parameter Σ, onto a sample characterized by $\hat{\sigma} = 3$

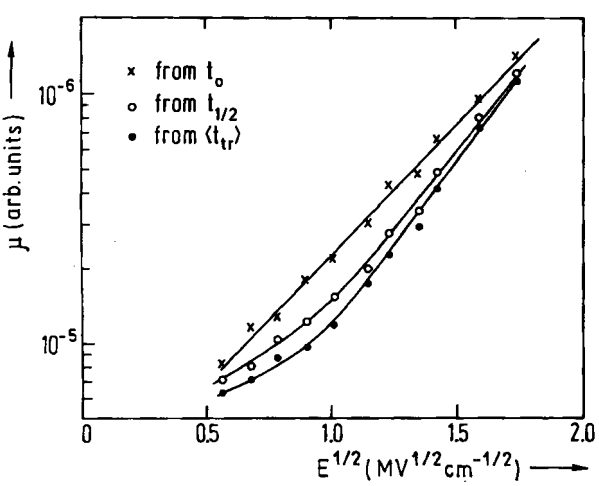

Fig. 9. $\ln \mu$ vs. $E^{1/2}$ plots of the carrier mobility based on different definitions of the transit time (from [64])

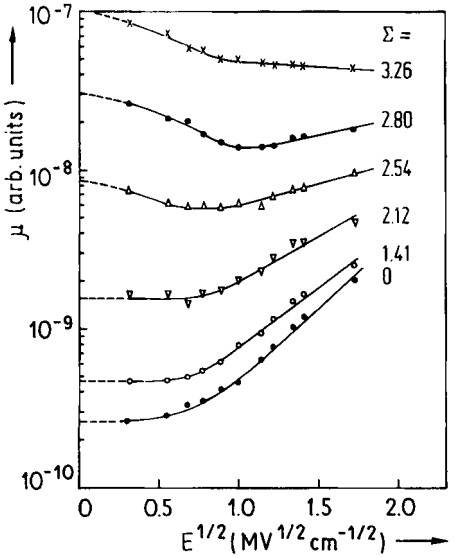

Fig. 10. Mobility μ vs. $E^{1/2}$ for a hopping system with fixed energetic disorder ($\hat{\sigma} = 3$) and variable off-diagonal disorder (from [61])

changes the $\mu(E)$ pattern in a characteristic way. With increasing Σ the low-field portion of $\mu(E)$ plots tends to bend upward yielding mobilities that increase with decreasing field. Within the $\ln \mu \propto E^{1/2}$ regime the values of the slope S decrease and eventually become negative (Fig. 10). This behavior can be explained in the following manner. Fluctuation of the overlap parameter Γ_{ij} about a mean value translates into asymmetric variation of the factor $\exp(-\Gamma_{ij})$ controlling the exchange rate of a charge carrier. The effect is reminiscent of percolation. While certain routes for a carrier will be blocked due to more unfavorable intersite coupling, easy channels are opened that overcompensate for the loss of the former. To first-order approximation one can describe the diffusion enhancement by replacing the distribution of overlap factors by the ensemble-averaged diffusion coefficient

$$\langle D \rangle \propto \langle \exp[-2g(\Gamma_i)] \rangle , \tag{12}$$

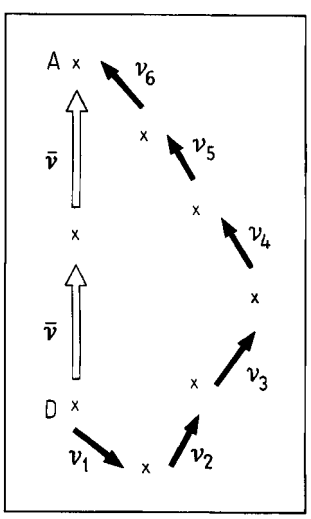

Fig. 11. Schematic view of the different routes a charge carrier can follow to move from D to A. If the electric field acts on the D–A direction the jump with rate ν_1 occurs against the field direction

where

$$g(\Gamma) = (\pi\Sigma)^{-1} \exp\left[-(\Gamma - \gamma a)^2/\Sigma^2\right] \tag{13}$$

is the Gaussian weight distribution of the coupling parameter of the individual sites (see Section 2). Averaging can be done analytically [65] and yields

$$\langle D(\Sigma)\rangle = D(\Sigma = 0) \exp\left(\tfrac{1}{2}\,\Sigma^2\right). \tag{14}$$

The microscopic aspect of the effect is illustrated in Fig. 11. While the direct path is impeded by poor overlap or larger distance the loop opens a detour that is faster because of improved coupling. Fig. 11 also provides a qualitative explanation for the negative effect of an electric field. Suppose the field acts along the direct path. A carrier following the loop will, therefore, have to execute a jump against the field direction. Consequently, the field tends to eliminate the faster detour route. This effect is reminiscent of the phenomenon of negative differential resistance in the literature on hopping conduction in amorphous semiconductors [66]. The basic idea proposed by Shklovskii and coworkers [67, 68] for rationalizing this effect is to invoke field-induced localization by traps or dead ends in a random network which for topological or energetic reasons can only be emptied by carrier jumps against the field direction. At low fields, where the heating effect of the field on the energetic distribution of hopping carriers is negligible, i.e. the regime of constant μ in a system with $\Sigma = 0$, it is basically this effect that is responsible for the decrease of μ with increasing E. At larger fields, depending on the magnitude of σ, it is overcompensated by the field effect on energy barriers along the field direction. It leads to an increase of μ with E, albeit weaker than in the absence of off-diagonal-disorder, but retaining the $\ln \mu \propto E^{1/2}$ relation. At very high fields the effective disorder seen by a migrating carrier va-

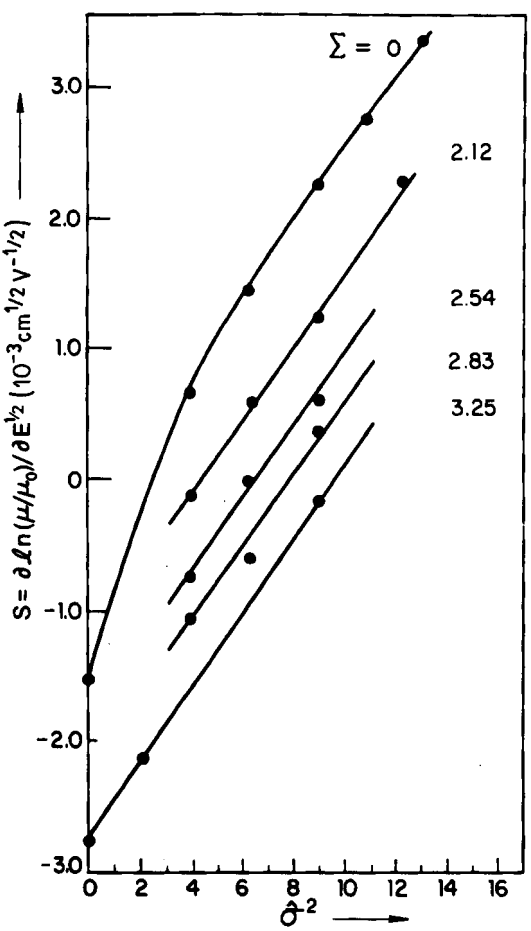

Fig. 12. The slope S of the $\ln \mu$ vs. $E^{1/2}$ plots versus $\hat{\sigma}^2$ parametric in Σ (from [30])

nishes and $\mu(E)$ must approach the $\mu \propto E^{-1}$ law expected for a pure hopping system in which backward transitions are excluded.

The quantity that is essential for analysing experimental $\mu(E, T)$ data is the dependence of S on the disorder parameters $\hat{\sigma}$ (i.e. temperature) and Σ. Fig. 12 shows simulation data for S plotted versus $\hat{\sigma}^2$ for various values of Σ. A family of parallel straight lines with slope $C = \partial S/\partial\hat{\sigma}^2 = 2.9 \times 10^{-4}$ (cm/Vs)$^{1/2}$ is recovered with systematic deviations occurring for $\hat{\sigma} < 2$. Plotting the values at which the field dependence of μ vanishes ($\hat{\sigma}^*$) as a function of Σ reveals a linear relationship for $\Sigma > 2$. The parameter $(\hat{\sigma}^*)^2$ levels off for $\Sigma < 2$ and attains an asymptotic limit of 1.5 (Fig. 13). If combined with the $\mu(T)$ relationship (11), a universal law is established relating μ to the degree of both diagonal and off-diagonal disorder in the high field limit,

$$\mu(\hat{\sigma}, \Sigma, E) = \mu_0 \exp\left(-\left(\tfrac{2}{3}\hat{\sigma}\right)^2\right) \begin{cases} \exp C(\hat{\sigma}^2 - \Sigma^2)\, E^{1/2}\,; & \Sigma \geqq 1.5\,, \\ \exp C(\hat{\sigma}^2 - 2.25)\, E^{1/2}\,; & \Sigma < 1.5\,. \end{cases} \tag{15}$$

Equation (15) is an approximation since the proper scaling quantity one had to use in the second exponential is the effective field $E^{\text{eff}} = eE\,\Delta x_{ji}/(2kT)$ rather than the applied electric field itself. While the dependence on the intersite distance can easily be taken into account via a concentration dependence of $C(C \propto c^{-1/6})$, the temperature dependence of E^{eff} should affect the functional T-dependence of $\mu(E, T)$. In practice corrections are expected to be small since the T^{-2}-dependence resulting from the $\hat{\sigma}^2$-term overrides the $T^{-1/2}$-effect due to E^{eff} except when $\hat{\sigma}^2 - \Sigma^2$ becomes very small. As far as the concentration dependence of C is concerned sample dilution to 30% transport sites would increase C by 18% only. Equation (15) accounts for the fact that $\mu(E)$ resembles the Poole-Frenkel behavior without requiring the presence of traps that are charged when empty, the slope S reversing sign at $\hat{\sigma} = \sigma^*(\Sigma)$. In accord with earlier conjecture [50] and with recent analytic theory [63] this effect, whose origin remained mysterious for a long time, is thus identified as a genuine

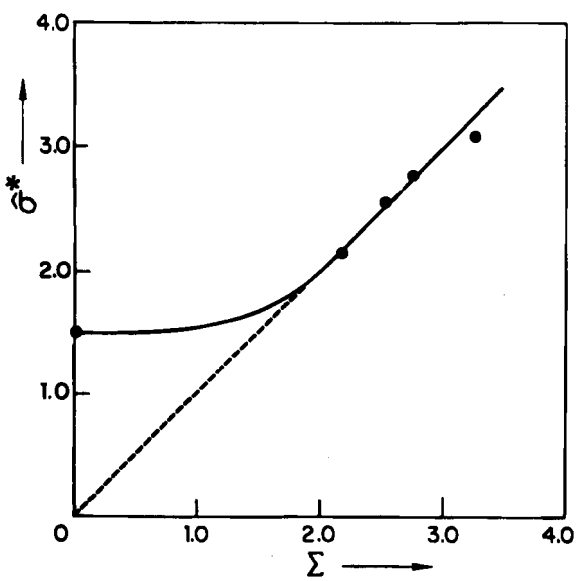

Fig. 13. The $\hat{\sigma}$-parameter at which the field dependence of the mobility vanishes ($\hat{\sigma}^*$) vs. Σ (from [30])

signature of hopping transport in a Gaussian DOS. Provided that the width of the DOS is temperature independent, which appears to be a reasonable approximation at temperatures sufficiently below the glass transition temperature, $\hat{\sigma}^*$ translates into a characteristic temperature $T^* = \sigma/k\hat{\sigma}^*$ which turns out to be the equivalent to the Gill temperature (see below). Note that (15) predicts a change of sign of the slopes of the $\ln \mu$ versus $E^{1/2}$ relationship even in the absence of off-diagonal disorder. Hence, an earlier statement made in [61] has to be modified in the sense that the presence of off-diagonal disorder suppresses the temperature at which the sign reversal occurs, yet is not a necessary condition for its observation. Neither has a temperature dependent decrease of S to be taken as evidence for a temperature dependence of Σ. If Σ increased with temperature, this would cause an increase of the slopes $\partial S/\partial\hat{\sigma}^2$ and $\partial S/\partial T^{-2}$, respectively.

It is useful to discuss (15) in conjunction with related formulae described in the literature. The first one is that of Gill [69], who proposed describing the temperature and field dependences of the mobility in poly-(N-vinylcarbazole) by the empirical formula

$$\mu(E, T) = \mu_0 \exp\left(-\frac{\Delta_0}{kT_{\text{eff}}}\right) \times \exp\left(\frac{\beta E^{1/2}}{kT_{\text{eff}}}\right), \tag{16}$$

where Δ_0 is a zero-field activation energy, μ_0 the pre-factor mobility, and T_{eff} is defined by $1/T_{\text{eff}} = 1/T - 1/T^*$. Gill selected this functional form to account for the fact that $\ln \mu(E, T)$ versus T^{-1} plots intersect at a finite temperature T^*. Equation (16) predicts that the field dependence becomes negative for $T > T^*$. This equation, however, has no theoretical justification.

In a study of hole transport in p-diethylaminobenzaldehyde-diphenylhydrazone-doped polycarbonate, Schein et al. [5] suggested factorizing the field and temperature dependences of the hole

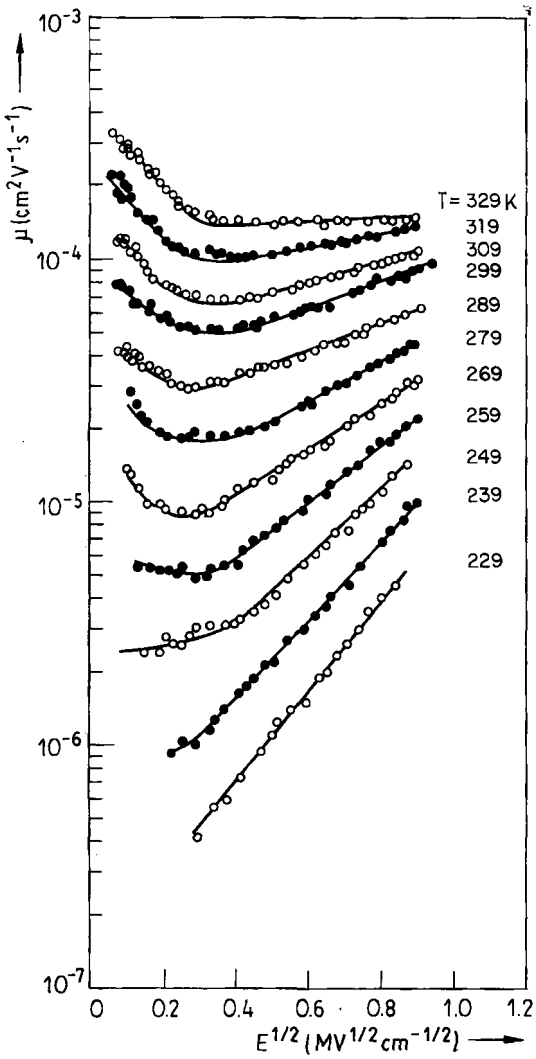

Fig. 14. Hole mobility in TAPC/polycarbonate against $E^{1/2}$, parametric in temperature (from [30])

mobility as

$$\mu(E, T) = \mu_0 \exp\left(-\left(\frac{T_0}{T}\right)^2\right) \exp\left(E^{1/2}\left(\frac{\beta}{T} - \gamma\right)\right). \tag{17}$$

Equation (17) predicts that the slopes of $\ln \mu$ versus $E^{1/2}$ plots become negative for $T > \beta/\gamma$. The constant β was found to agree within a factor of 2 with the Poole-Frenkel coefficient, while γ was an empirical parameter.

More recent studies of hole transport in tri-p-tolyamine-doped polycarbonate by Borsenberger [7] confirmed the validity of (17) if modified by replacing $1/T$ in the exponent of the field term by $(1/T)^2$. The present simulations substantiate this reasoning by demonstrating that a mobility obeying (17) is an inherent signature of the random walk of the carriers in a random potential with random electronic coupling under a bias field. This provides a means for determining the degree of built-in diagonal and off-diagonal disorder from $\mu(E, T)$ data.

A textbook example for the observation of the $\mu(E, T)$ behavior outlined above is the work of Borsenberger et al. [30] on hole transport in a TAPC polycarbonate composite (Fig. 14). Low-field (1×10^5 V cm^{-1}) mobility data follow (9) yielding $\sigma = 0.095$ eV for the width of the DOS and $\mu_0 = 2 \times 10^{-2}$ cm^2 V^{-1} s^{-1}. Knowing σ allows plotting the slope values of the $\ln \mu$ versus $E^{1/2}$ section of $\mu(E)$ plots versus $\hat{\sigma}^2$. For $\hat{\sigma}^2 > 14$ a straight line with slope $C = 3.0 \times 10^{-4}$ (cm/V)$^{1/2}$ is obtained in excellent agreement with simulation results (Fig. 15). The intersection of the extrapolated $S(\hat{\sigma}^2)$-line with $S = 0$ occurs at $(\hat{\sigma}^*)^2 = 9.6$ yielding an off-diagonal disorder parameter $\Sigma = 3.1$.The increase of the slope, $\partial S/\partial \hat{\sigma}^2$, noted as S approaches zero indicates that for $\hat{\sigma} < 3.75$, equivalent to $T \geqq 293$ K, Σ begins to increase. The most plausible explanation is that there is a thermally induced contribution of off-diagonal disorder in addition to the contribution due to the built-in compositional or geometrical disorder. The deviation of S versus $\hat{\sigma}^2$ from linearity could, in principle, also indicate the onset of a temperature-induced broadening of the DOS. However, the absence of a change of slope of $\mu(T)$ argues against this possibility.

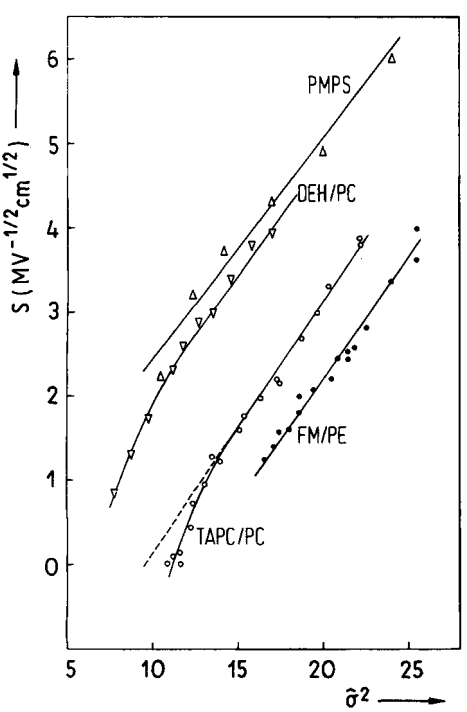

Fig. 15. The slope S of $\ln \mu$ vs. $E^{1/2}$ plots for various experimental systems. Data are from [29] (PMPS), [5] (DEH/polycarbonate), [30] (TAPC/PC), and [96] (FM/PE, (4-n-butoxycarbonyl-9-fluovenylidene)-malonitrile doped into polyester)

A stringent test for the applicability of the MC results to analyse those data is the occurrence of the increase of μ at low fields predicted for $\Sigma \approx 3$. Unfortunately, the dramatic increase in computer time prevents collecting MC data for both large $\hat{\sigma}$ and Σ at low fields. From Fig. 7 and 10 it is, nevertheless, obvious that the general trend borne out by the data of Fig. 14 is recovered.

To document that the above behavioral pattern is indeed a universal feature of transport in molecularly doped polymers and main chain polymers like poly(methylphenylsilane) representative data for $S(\hat{\sigma}^2)$ are collected in Fig. 15. Apart from their bearing out the same functional pattern, the slope parameters C agree within 20% with the simulation value. The various systems differ with regard to the degree of off-diagonal disorder which is likely to be related to intermolecular packing constraints affecting both the average electronic coupling among the sites as well as its fluctuation. Note that the PMPS data suggest $\Sigma \approx 0$ in accord with the absence of a mobility increase at low fields (Fig. 8).

4.4 Anomalous broadening of time of flight signals

In conventional Gaussian transport the ratio of diffusive spread Δx of an initially δ-shaped carrier sheet to its displacement x is

$$\frac{\langle \Delta x^2 \rangle^{1/2}}{\langle x \rangle} = \frac{kT}{eE}\left(\frac{2}{Dt}\right)^{1/2}. \tag{18}$$

This implies validity of Einstein's law relating diffusivity to mobility via $eD = \mu kT$. For an applied voltage $U = 500$ V at 290 K a relative spread of the transit time $\Delta t_{tr}/t_{tr} = (2kT/eU)^{1/2}$ of order 10^{-2} is obtained. The experimentally observed spreadings of the tails of what appears to be non-dispersive TOF signals are much larger [31]. This must be the result of non-thermal field-assisted spreading of the drifting carrier packet due to disorder. It is obvious from Fig. 16 showing a series of TOF signals parametric in $\hat{\sigma}$ at vanishing off-diagonal disorder that this effect is recovered by simulation [64]. The spread of the tail, quantifiable via the dispersion

$$w = \frac{t_{1/2} - t_0}{t_{1/2}} = \left(\frac{\pi D}{\mu E L}\right)^{1/2}, \tag{19}$$

increases with increasing disorder (for definition of t_0 and $t_{1/2}$ see Section 4.3).

The spreading of TOF signals can be accounted for by defining a diffusivity that consists of the ordinary thermal term D_0 and a field- and disorder-dependent contribution $D_f(\hat{\sigma}, E)$. The latter can be determined from the spatial variance of the carrier packet in field direction, yielding

$$\frac{e}{\mu kT}\,\frac{\langle (x - \langle x \rangle)^2 \rangle}{2t} = f(E) = 1 + \frac{eD_f}{\mu kT}. \tag{20}$$

The quantity $f(\hat{\sigma}, E) - 1$ thus measures the deviation of a random hopping system under an applied bias field from conventional Einstein behavior. Data for $f(\hat{\sigma}, E) - 1$ bear out a quadratic relationship on the electric field in the field range 10^5 to 10^6 V cm^{-1} as long as $\hat{\sigma} \leqq 3$ and $\Sigma = 0$. At still larger fields $f(\hat{\sigma}, E) - 1$ levels-off and begins to decrease (Fig. 17). This is a consequence of the gradual reduction in the effective disorder a random walker experiences when migrating in a random potential strongly tilted along the field direction.

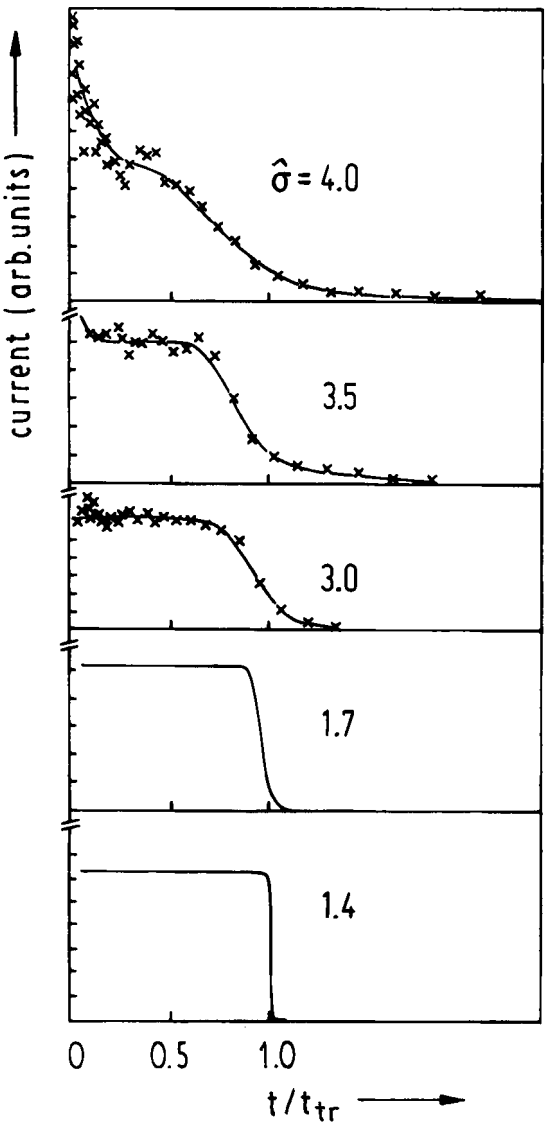

Fig. 16. Time of flight (TOF) signals, parametric in $\hat{\sigma}$ (example length 8000 lattice planes, $E = 6 \times 10^5$ V cm^{-1})

For $E \to \infty$ all states become available, implying that the effect of disorder vanishes and $f(\hat{\sigma}, E)$ approaches its thermal value which itself is field dependent, however. In a hopping system with no disorder $D \propto \cosh eEa(2kT)$ and the drift velocity increases as $v = \mu E \propto \sinh eEa/(kT)$ yielding $D(\hat{\sigma} = 0, E) - 1 = x \operatorname{cotan} x \approx x^3/3$ with $x = eEa/(2kT)$. The simulation data fort $\hat{\sigma} = 0$ are consistent with this analytic result (Fig. 17).

For $\hat{\sigma} = 3.5$, which turns out to be an experimentally relevant disorder parameter, $f(E) - 1$ approaches an approximately linear field dependence over an appreciable field range. By means of (19) it is immediately seen that this gives rise to universality of TOF signals that are non-dispersive, i.e., exhibit a well-developed plateau and yield a thickness-independent carrier mobility. Recall that in the past universality has been considered as a hallmark of dispersive transport treated in terms of Scher-Montroll theory [21, 70]. The Monte Carlo simulation results demonstrate that this is all but so: Universality is a signature of quasi-equilibrium stochastic hopping motion within a sufficiently wide Gaussian DOS under the action of a drain field. This is confirmed by experiments which often yield universal yet non-dispersive TOF signals [71, 86] and by simulation [64].

Since the quantity directly accessible by experiment is the dispersion w of a TOF pulse it seems appropriate to outline the prediction of Monte Carlo simulation as far as the dependences of w on electric field an sample length L are concerned for systems with superimposed diagonal and off-diagonal disorder. Fig. 18 illustrates how the functional dependence of w on E changes from $w \propto E^{1/2}$ at small disorder to $w \approx$ const at larger disorder. At $E \geqq 10^6$ V cm^{-1} w decreases because the effective energetic disorder experienced by a drifting carrier is significantly reduced as eEa becomes comparable to σ.

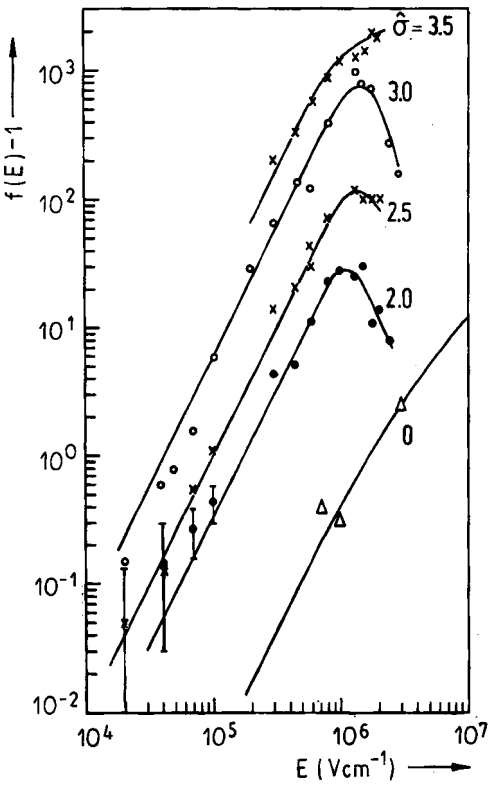

Fig. 17. $f(E) - 1$ against electric field, parametric in $\hat{\sigma}$ (from [64])

An interesting phenomenon is observed concerning the evolution of the spatial variance of a packet of carriers as a function of its position within the sample. This allows calculating w as a function of L. Fig. 19 presents data for w at variable $\hat{\sigma}$, $\Sigma = 0$, and $E = 6 \times 10^5$ V cm^{-1}. w turns out to be independent of L at short L and starts decreasing as $w \propto L^{-1/2}$ above a critical length that increases with increasing $\hat{\sigma}$. Extrapolating w normalized to the dispersion w_0 expected for $\hat{\sigma} = 0$ allows predicting the break in $w(L)$ plot for larger disorder parameters and larger samples, respectively. TOF signals are thus expected to be universal for $L \leqq 20$ μm provided that $\hat{\sigma} \geqq 4$. Remarkably, experimental data taken by Young [72] in a 30% DEH/polystyrene sample, known to contain only a small degree of built-in off-diagonal disorder, yield $w = 0.4$ for $4\,\mu\text{m} \leqq L \leqq 40\,\mu\text{m}$ indicating that $\hat{\sigma}$ must be ≈ 4.2 at 295 K, equivalent to $\sigma > 0.11$ eV. This is consistent with the temperature dependence of the hole mobility yielding $\sigma = 0.13$ eV [73]. On the other hand, the $w(L)$ data of Yuh and Stolka [31] on 40% TPD/polycarbonate bear out a $L^{-1/2}$ dependence (see Fig. 19) as expected for $\hat{\sigma} = 4.0$, while the $\hat{\sigma}$-value inferred from the $\mu(T)$-data is 4.2 ($\sigma = 0.108$ eV). Considering the uncertainty in the extrapolation the agreement is remarkably good. It confirms that the scaling behavior of w, notably the change in the functional dependence at large L from $w \neq f(L)$ to $w \propto L^{-1/2}$ is a characteristic feature of hopping motion within a Gaussian DOS. The $w \propto L^{-1/2}$ behavior indicates that the ultimately the long-time limit has been attained although the spatial variance of the carrier packet maintains being anomalously large.

In order to determine whether or not off-diagonal disorder has the same effect on $w(L)$ as energetic disorder a series of computations were carried out for various superpositions of energetic and geometric disorders. The result shown in Fig. 20 indicates that the latter does contribute to the spreading of TOF signals, yet does not yield $w \neq f(L)$ with samples of macroscopic length unless a significant amount of energetic disorder is superimposed.

Another way of demonstrating the success of the disorder model to account for the temporal features of a TOF signals is to compare experimental TOF signals with Monte Carlo simulations based upon the disorder parameters inferred from the dependences of μ on temperature and electric field. This is illustrated in Fig. 21 and 22 for a pure TAPC glass and 75% TAPC/PC. The agreement is striking.

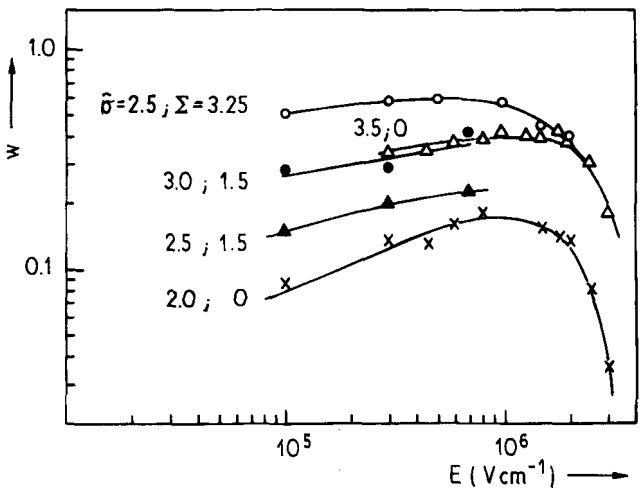

Fig. 18. Dispersion w vs. electric field for various combinations of diagonal and off-diagonal disorder. (The sample length was 8000 lattice planes)

For the interpretation of field-induced spreading of TOF tails it is important to note that it is not due to topological memory effects a random walker may be subject to. Simulations carried out on systems whose site energies were redefined after each jump yielded virtually identical results [64]. This demonstrates that the effect is related to the distribution of jump rates as an inherent feature of hopping transport in random media. Recall that ordinary diffusive broadening of a sheet of charge carriers drifting under the action of a bias field follows Einstein's law relating diffusivity and mobility only if the field

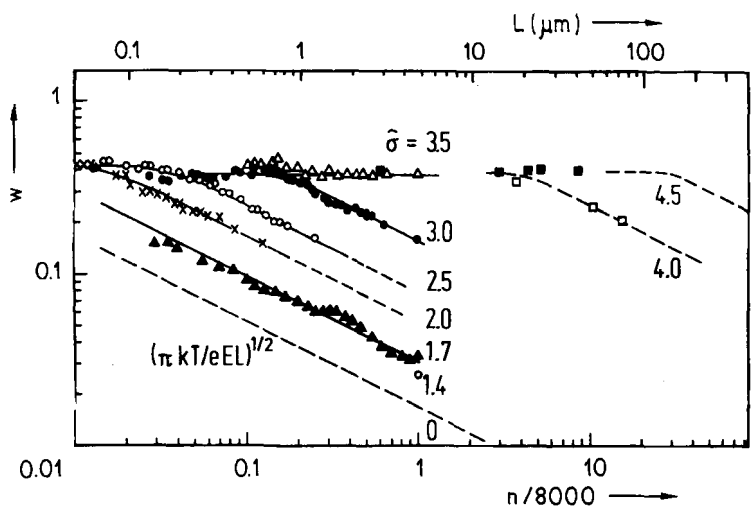

Fig. 19. Simulation result for w vs. normalized sample length. Dashed curves are extrapolations. Experimental data are for 30% DEH doped into polystyrene (full squares) (from [72]) and for 40% TPD doped into polycarbonate (open squares) (from [31])

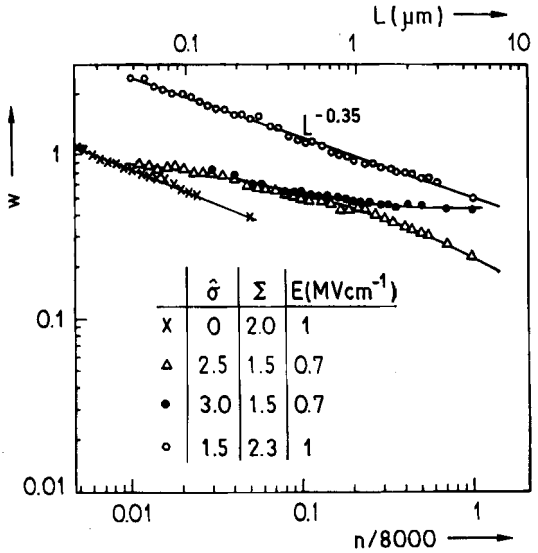

Fig. 20. w as a function of normalized sample length for various combinations of diagonal and off-diagonal disorder and electric field

is small, i.e. $eEa/(2kT) \ll 1$, and if the medium is homogeneous. The latter condition requires that, in the case of incoherent hopping transport, the jump rate be a well-defined quantity. It is violated in an energetically or positionally disordered medium. In Section 4.1 it has been described that carriers executing a random walk in a Gaussian DOS tend to settle on average at an energy $-\sigma^2/(kT)$ below its center, the variance of the occupational DOS

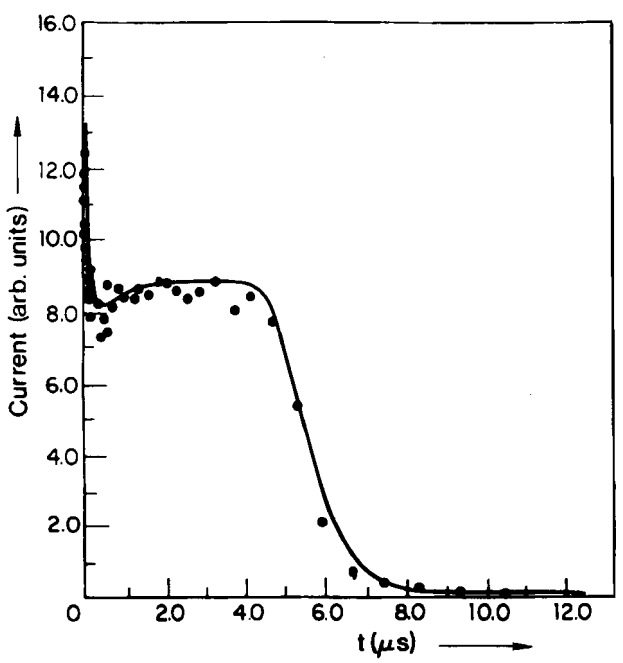

Fig. 21. A comparison of the experimental TOF signal (———) for an amorphous TAPC layer with the simulation result (●) for $\sigma = 0.067$ eV, $T = 295$ K, and $\Sigma = 2.12$ (from [60])

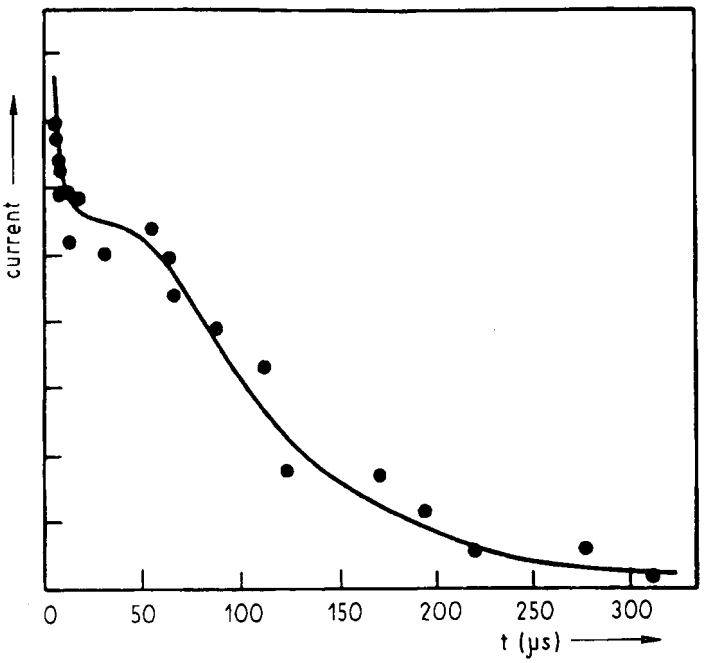

Fig. 22. A comparison of a TOF signal (———) recorded with a TAPC/PC sample and the simulation result (●) for the parameters $\hat{\sigma} = 3.5$ and $\Sigma = 3.25$ that follow from the analysis of $\mu(E, T)$ data (from [30])

being σ. The jump rate of carriers temporarily localized in the bottom states of the DOS^{occ} will, therefore, be lower than average and vice versa. The concomitant distribution of jump rates must give rise to non-thermal spatial spreading of the carrier packet if subject to an applied drain field. Since no field is acting in perpendicular direction, the shape of the carrier packet becomes cigar-like. A similar effect was first noticed by Rudenko and Arkhipov [74] when analysing transport of charge carriers subject to multiple trapping (MT) by a Gaussian distribution of trap levels and later on by Bouchaud and Georges [75] in the course of their analytic study of hydrodynamic flow in porous media. An elaboration of the MT case has recently been given by Haarer et al. [49]. Despite the similarities between MT and hopping in a distribution of intrinsic hopping states derived from the band states via disorder-induced localization, there are essential differences involved in both approaches as discussed in greater detail in [64].

4.5 Transition from non-dispersive to dispersive transport

Since the time a packet of carriers, started randomly in energy, needs to relax to dynamic equilibrium increases faster with time than the transit time across a sample (see Section 4.1), TOF signals must eventually become dispersive once the temperature drops below a certain value that depends on the width of the DOS. To delineate the general phenomenological pattern, a series of double logarithmic current versus time plots, parametric in $\hat{\sigma}$, covering up to 20 decades in time and up to 10 decades in amplitude are presented in Fig. 23. The curves for $\hat{\sigma} = 3$, 6, and 8 represent the results of an analytic effective medium

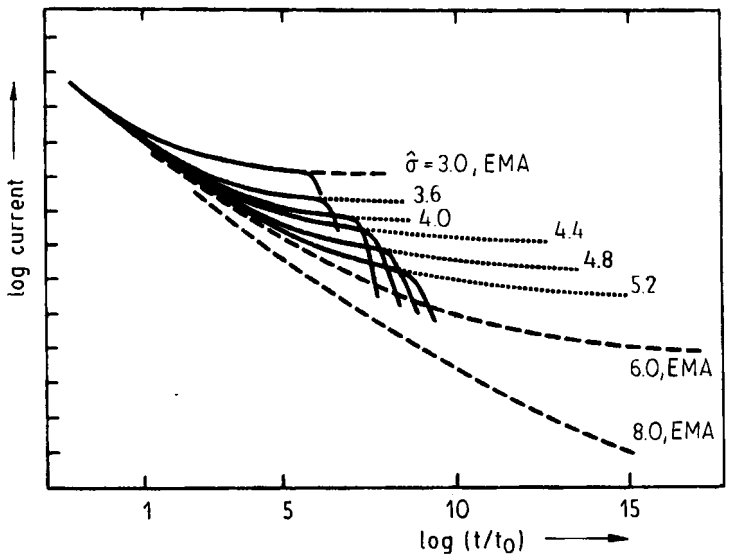

Fig. 23. Double logarithmic current vs. time plots. The full and dotted curves are simulation results and their extrapolations towards equilibrium. The dashed curves are the result of the effective medium approximation for an infinite sample (from [76])

(EMA) calculation of the zero-field diffusivity of a packet of carriers in an infinite sample [45]. Apart from demonstrating the mutual consistency of EMA and simulation results, these plots indicate that in no case a simple power law of the type $i(t) \propto t^{-(1-\alpha)}$ is obeyed for times less than the mean arrival time $\langle t_T \rangle$. At short times the time dependence of the current is virtually independent of $\hat{\sigma}$ but tends to saturate earlier with decreasing $\hat{\sigma}$.

A more detailed family of current transients, parametric in $\hat{\sigma}$, is shown in Fig. 24 for a sample with $n_z = 4000$, equivalent to a thickness of 2.4 μm. The occurrence of a ND → D transition with increasing $\hat{\sigma}$ is obvious. While the transients reveal a plateau of variable temporal length for $\hat{\sigma} < 4$, this is no longer the case for $\hat{\sigma} > 4.4$. Reducing the sample length at fixed $\hat{\sigma}$ causes the initial portion of the transients to appear more dispersive. This is shown in Fig. 25. The ND → D transition is more clearly delineated by plotting the reciprocal mean carrier arival time as a function of $\hat{\sigma}^2$, parametric in sample length, and the arrival time as a function of n_z at variable $\hat{\sigma}$, as shown in Fig. 26 and 27, respectively. Within the dispersive regime, $t_T(n_z)$ deviates from linearity, $\langle t_T \rangle \propto n_z^m$, where $1.25 < m < 1.40$ for $4.0 < \hat{\sigma} < 5.2$. At the same time, $L/(E\langle t_T \rangle)$ exceeds the value predicted by the dependence of the mobility on the disorder parameter at moderate fields, $\mu(\hat{\sigma}) = \mu_0 \exp(-(2\hat{\sigma}/3)^2)$ and $\hat{\sigma} \leqq 4$ (see Section 4.2). Instead, $\langle t_T \rangle^{-1}$ varies approximately as $\exp(-(\hat{\sigma}/2)^2)$.

In previous studies, the onset of dispersion has been defined by the condition that the current no longer decays to a plateau value for $t < \langle t_T \rangle$. Operationally, the time at which the current becomes time independent turned out to be about one tenth of the time a packet of carriers needs to equilibrate energetically within a Gaussian DOS [52]. Fig. 26 offers a criterion for the occurrence of the ND → D transition that alleviates the problem of having to define the time at which the current becomes constant. It indicates that below a critical value of the disorder parameter, $\hat{\sigma}_c$, the mobility derived from the mean carrier arrival time is independent of thickness, thus reflecting a genuine material property. In this sense, the

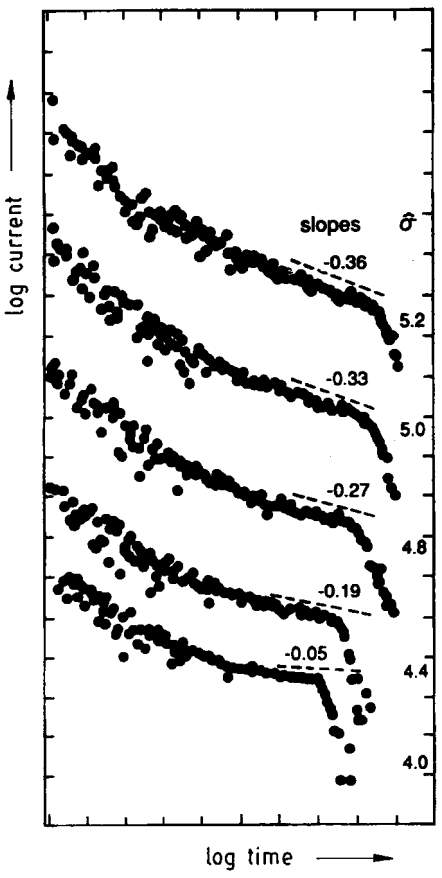

Fig. 24

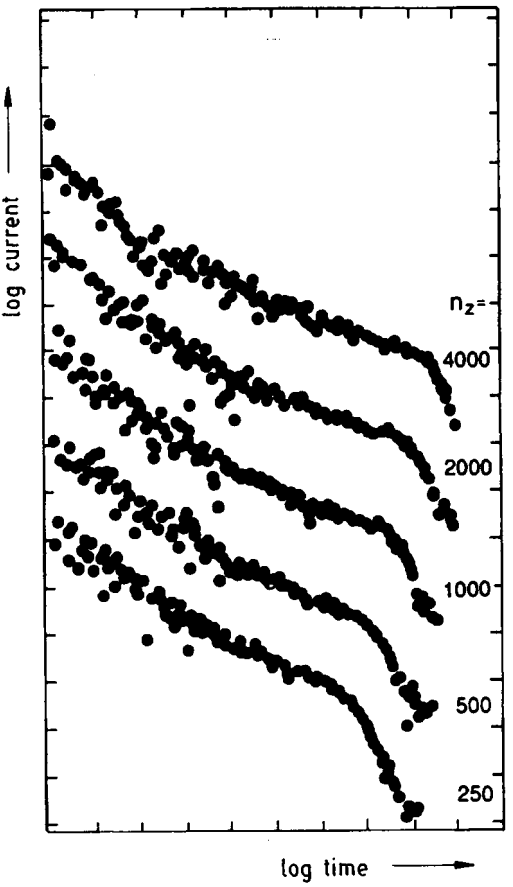

Fig. 25

Fig. 24. Simulated transients, parametric in $\hat{\sigma}$ for a sample consisting of $n_z = 4000$ lattice planes, $E = 0.6$ MV cm^{-1} (from [76])

Fig. 25. Simulated TOF signals, parametric in n_z with $\hat{\sigma} = 5.2$, $E = 0.6$ MV cm^{-1} (from [76])

ND → D transition separates a transport regime in which the mean carrier arrival time yields a thickness-independent transport coefficient from a regime in which this is no longer the case. Operationally, the ND → D transition can be defined via the intersection of the $\log \langle t_T \rangle$ versus $\hat{\sigma}^2$ lines representing the average reciprocal carrier arrival times in the non-dispersive and dispersive regimes, respectively. This yields a correlation between the critical disorder parameter, $\hat{\sigma}_c$, and sample length. Fig. 28 indicates that the critical disorder parameter at which the ND → D transition occurs increases with the number of lattice planes as $\hat{\sigma}_c^2 = A + B \log n_z$, where $A = -3.6$ and $B = 6.7$ are empirical constants, equivalent to

$$\hat{\sigma}_c^2 = A' + B \log L , \tag{21}$$

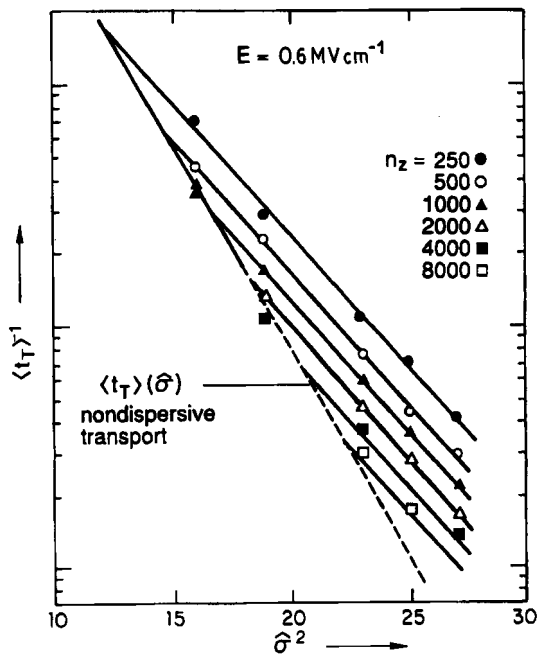

Fig. 26. Simulated reciprocal mean arrival times vs. $\hat{\sigma}^2$, parametric in n_z (from [76]). The asymptote describing non-dispersive transport was taken from [30]

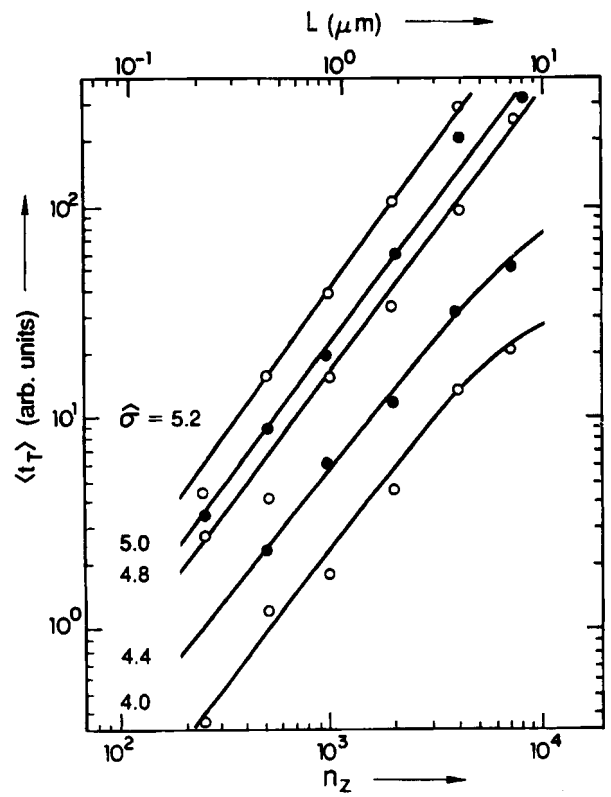

Fig. 27. Simulated mean arrival times vs. n_z, parametric in $\hat{\sigma}$ (from [76])

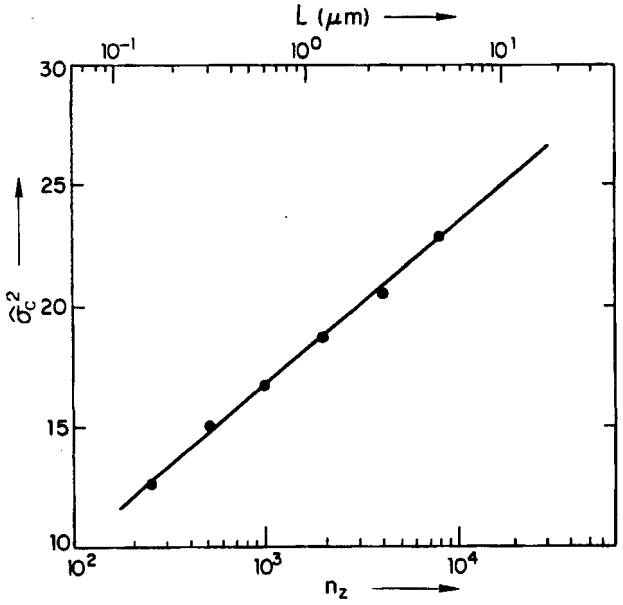

Fig. 28. The disorder parameter at which the ND → D transition occurs vs. sample length

where $A' = 44.8$ and L is the sample thickness in cm. With a thickness of 20 μm and a DOS width of 0.1 eV, transients are then predicted to be dispersive at 232 K. According to a simple criterion used earlier [52], a temperature of 286 K would have been estimated.

A transient at $\hat{\sigma} = \hat{\sigma}_c$ does reveal an inflection if plotted on a double-linear scale, yet not a well-developed plateau. This is illustrated in Fig. 29 showing a transient for $n_z = 8000$ at $\hat{\sigma} = 4.8$ which is very close to $\hat{\sigma}_c$. Obviously, transients that appear moderately dispersive on double-linear scales featuring a slope $-(1 - \alpha_1) \approx 0.27$ in double-logarithmic representation are still satisfactory for determining mobilities that represent bulk properties. One reason is that the inflection monitors the arrival of the fastest equilibrating earlier, while re-

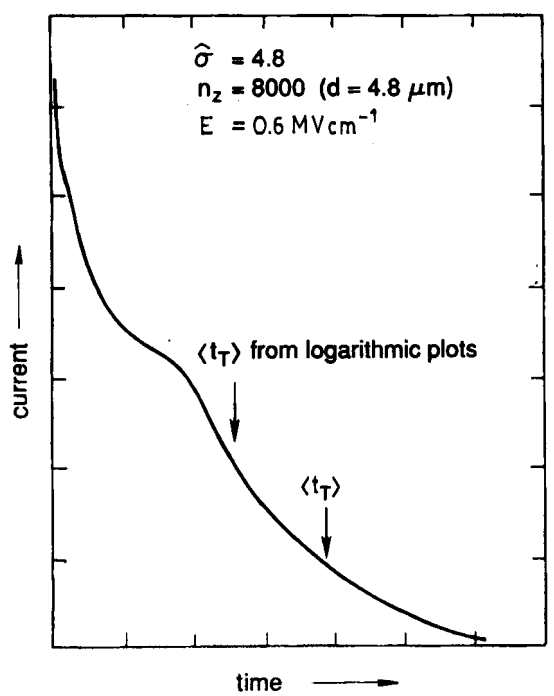

Fig. 29. Simulated TOF signal at the ND → D transition

sidual current relaxation is controlled by slower carriers hopping within the bottom part of the occupational DOS. Fig. 29 also illustrates that the absolute magnitude of the mobility may differ up to a factor of 2 depending on how the arrival time is defined. Inferring $\langle t_T \rangle$ from the intersection of asymptotes in double-linear plots, which is the common experimental practice, yields values that are approximately a factor of 2 larger than values derived from $\langle t_T \rangle$ which, unfortunately, are not directly accessible in experiment. Another reason why σ_c is larger than previously [52] assumed is related to the effect an electric field has on the relaxation behavior of carriers within a Gaussian DOS. A field raises the equilibrium energy of carriers within the DOS and, concomitantly, shortens the equilibration time.

Following Scher and Montroll [21] it has become practice to analyse dispersive TOF signals in terms of the algebraic decay functions

$$i(t) \propto \begin{cases} t^{-(1-\alpha)}; & t < t_T, \\ t^{-(1+\alpha)}; & t > t_T. \end{cases} \tag{22}$$

From Fig. 22 the failure of (22) for rationalizing dispersive transients in a material with a Gaussian DOS is obvious. Operationally, one can, nevertheless, determine a dispersion parameter from the current transient in double-logarithmic representation within, say, the last one and a half decades in time prior to the inflection because the curvature is small on this time scale. Fig. 30 presents experimental (see below) as well as simulation data for the related slope $-(1 - \alpha_1)$ of the double-logarithmic curves for $t < \langle t_T \rangle$. Empirically, $-(1 - \alpha_1) \propto (\hat{\sigma} - 3.9)^{3/4}$.

The parameter α_1 may be used to characterize a dispersive transient, although it must not be considered as the dispersion parameter in the sense of the Scher-Montroll (SM) theory implying that it can be recovered from different functional dependencies. The failure of this procedure can be illustrated by the following argument.

(i) SM theory predicts $\langle t_T \rangle \propto (d/E)^{1/\alpha}$. Simulated transients do, in fact, bear out a superlinear dependence of $\langle t_T \rangle$ on sample length, as shown in Fig. 27, However, α-values turn out to be larger than α_1.

(ii) According to SM theory, slopes of double-logarithmic plots should add to 2, implying that in the time domains $t \lesssim \langle t_T \rangle$ the decay of the current is controlled by the same α. Fig. 30 contradicts this prediction. Despite considerable data scatter, it is obvious that α_2 inferred from the tail of the double-logarithmic plots always exceeds α_1. This is a common observation, frequently encountered in analysing dispersive transients in disordered molecular solids, and no general solution to the problem has been offered thus far. The present work demonstrates that it is a signature of the inapplicability of (22), in particular of the fact that the dispersion parameter is not a good statistical quantity for describing transport processes.

These results demonstrate that the scaling behavior considered, to be a hallmark of dispersive transport, is not, or at best in zero-order approximation fulfilled in the case of hopping within a Gaussian DOS before attainment of dynamic equilibrium. Scaling is the consequence of an algebraic waiting time distribution, $\psi(t) \propto t^{-(1+\alpha)}$, with α being independent of time. This is realized in materials in which multiple trapping within an exponential trap distribution prevails. Hopping within a Gaussian DOS, which is the signature of organic glasses and molecularly doped polymers, does not fall into this category. One can rationalize the violation of scaling in terms of the energy relaxation function. In the case of multiple trapping or, equivalently, hopping in an exponential DOS, energetic

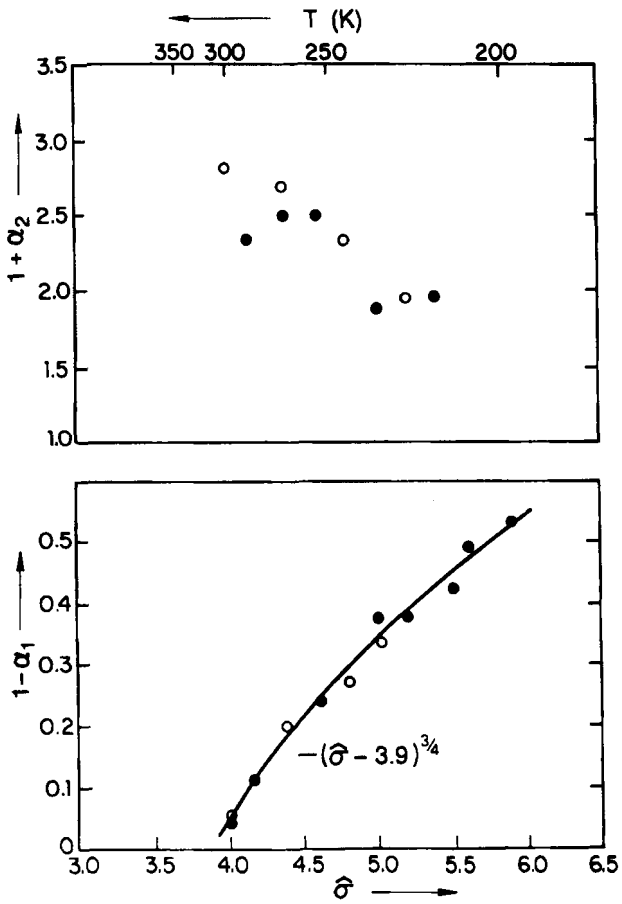

Fig. 30. Simulated (solid circles) and experimental (open circles from Fig. 31) values for the slope parameters of Scher-Montroll plots

relaxation of an ensemble of excitations strictly follows a logarithmic time dependence, independent of the absolute time scale. Changing the experimental time scale by varying the sample thickness or the field will not, therefore, change the relaxation pattern. Concomitantly, current transients are universal on a double-logarithmic scale. For a Gaussian DOS, the energy relaxation function is no longer linear on a logarithmic scale but tends to settle at a mean energy $-\sigma^2/kT$ below the center of the DOS. Changing the time scale by varying either the sample length or the field will therefore alter the relaxation pattern via the interplay of two opposing effects. Reducing the length will shift the relaxation pattern into a time domain in which $\partial\, \Delta E/\partial \ln t$ is larger, i.e. render the transients more dispersive. On the other hand, increasing the electric field will raise the mean equilibrium energy of carriers with the consequence that equilibrium is attained faster.

A textbook example of the success of the disorder formalism to predict the temperature dependence of the shape of progressively dispersive TOF signals on the basis of the energetic disorder parameter determined from high-temperatur $\mu(T)$ data is the recent work by Borsenberger et al. on a neat DEH glass [76]. A series of experimental TOF signals is shown in Fig. 31 on both double-linear and double-logarithmic scales, respectively. The

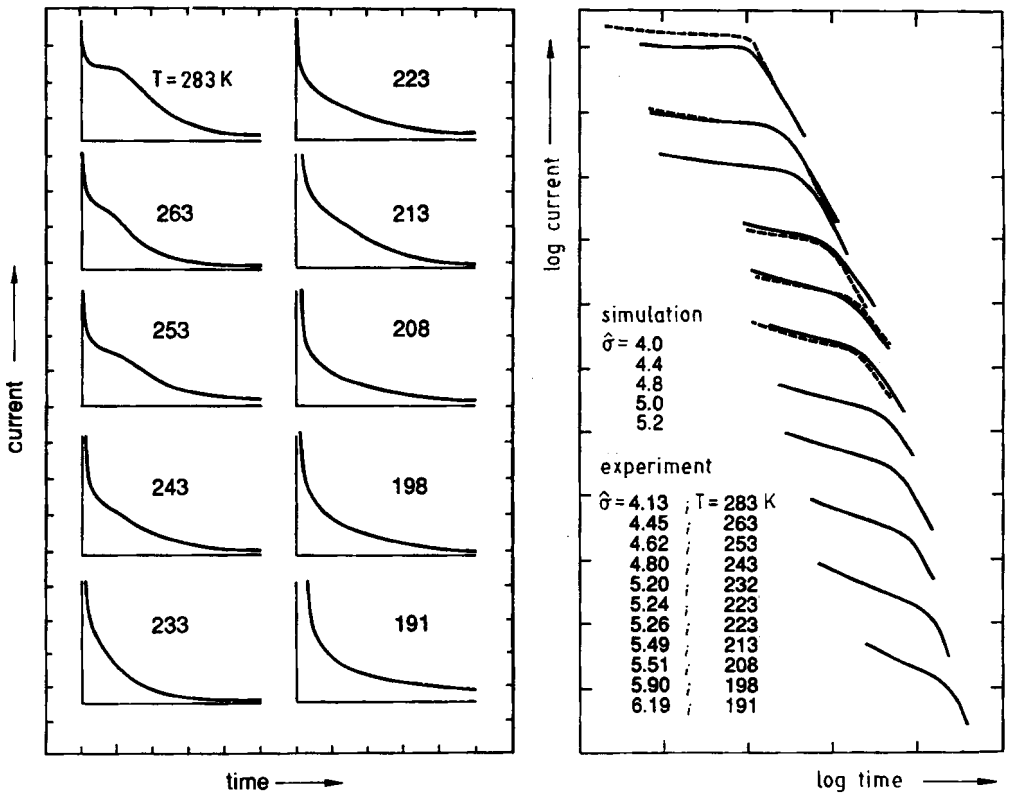

Fig. 31. a) Experimental TOF signals measured with a 5.6 μm thick amorphous DEH film at various temperatures ($E = 0.6$ MV cm^{-1}). b) The same transients in double-logarithmic representation. The dashed curves are simulations based upon a width of the DOS of $\sigma = 0.101$ eV. The experimental transient for $\hat{\sigma} = 4.45$ is coincident with the simulation for $\hat{\sigma} = 4.4$ (from [76])

latter diagram contains simulated TOF signals based upon $\sigma = 0.101$ eV as inferred from the $\mu(T)$ data. Note that there is no adjustable parameter except the trivial scaling factor relating the time frame of the simulation to the experimental time frame. Not only is the agreement betwen experiment and simulation a crucial consistency test of the model, it also demonstrates that for this system the entire T-dependence of μ must be attributed to disorder. Would it contain a polaronic contribution the onset of dispersion should have occurred at lower temperatures than observed. The ND → D transition is also evident from a plot of the mobility versus $\hat{\sigma}^2$ for two different sample thicknesses (Fig. 32). The predicted thickness-dependent kink occurs in quantitative accord with model predictions.

Superposition of any additional disorder, such as positional disorder or trap-capturing involving a distribution of traps, causes further broadening of the tails of dispersive TOF signals without changing the behavioral pattern in general [77]. This is evident by comparing the TOF signals Müller-Horsche et al. [20] reported for PVK with the simulation results. Translating the activation energy of the "mobility" Pfister and Griffith [78] measured for PVK into a width of the DOS yields $\sigma = 0.11$ eV. This allows plotting their $1 - \alpha_1$ and $1 + \alpha_2$ data versus $\hat{\sigma}$ (Fig. 33). While the $1 - \alpha_1$ values are close to the simulation

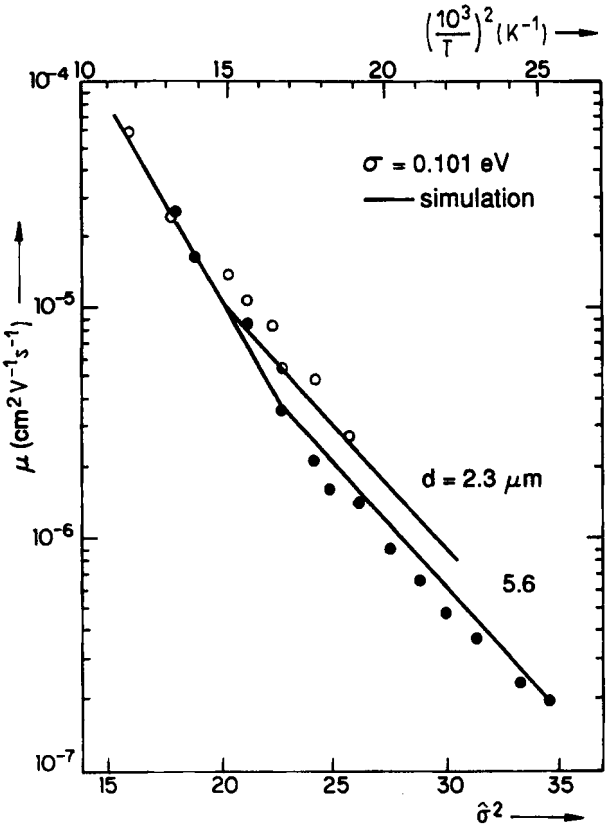

Fig. 32. Hole mobilities, operationally defined as $\mu = L/E\langle t_{tr}\rangle$, for DEH samples of different thicknesses (from [76])

results, $1 + \alpha_2$ is smaller by about 0.5. This is readily accounted for in terms of trapping by carbazole sandwich pairs causing stretching of TOF tails. The results are similar to more recent ones obtained for TAPC/PC [77] in which geometric disorder in addition to energetic disorder is significant.

4.6 Concentration dependence of μ

For technological reasons the dependence of the charge carrier mobility on the concentration of the transport moiety in molecuarly doped polymers has been the subject of early and intense research in this field. It is obvious that μ must decrease as the system of transport sites is diluted. On the other hand, dilution prevents aggregation of the photoconductor and improves the mechanical properties of the film which are largely controlled by the polymeric binder. A compromise has, therefore, to be made concerning the optimum concentration of the charge transporting species based upon knowledge of $\mu(c)$.

Experimentally, μ is found to decrease by some five orders of magnitude within the relative concentration range $1.0 \geqq c \geqq 0.1$ [1, 4, 79] (c is the volume fraction of the transporting material). The simplest way to understand this effect is in terms of the homogeneous lattice model [22, 51, 69, 80]. One assumes that the only effect of dilution is to increase the mean

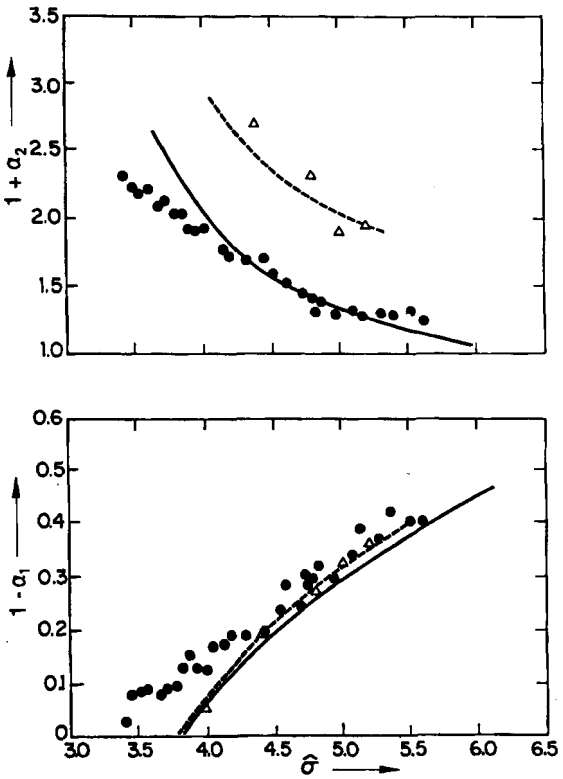

Fig. 33. Comparison of $1 - \alpha_1$ and $1 + \alpha_2$ for PVK measured by Pfister and Griffith [78]. The plot vs. $\hat{\sigma}$ is based upon a width of the DOS of $\sigma = 0.11$ eV derived from their $\mu(T)$ data. The dashed line (fitting the triangles) is the simulation result for a system with energetic disorder only

distance among transporting molecules according to

$$\langle R \rangle = ac^{-1/3}, \tag{23}$$

where a is the mean nearest neighbor distance in the undiluted system. Within the framework of the concept of incoherent transport this has two consequences: (i) the wave function overlap factor decreases with increasing c according to $\exp(-2\gamma ac^{-1/3})$ and (ii) the mean square displacement per jump increases proportional to $c^{-2/3}$. Hence, the prefactor of the mobility becomes

$$\mu_0(c) = a_0 c^{-2/3} \exp(-2\gamma ac^{-1/3}), \tag{24}$$

where $a_0 = (e/kT)(a^2 v_0/6)$, v_0 being the prefactor in the expression for the jump rate (2). The full expression for μ is

$$\mu(E, T, c) = \mu_0(c) f_1(T, c) f_2(E, T, c), \tag{25}$$

where f_2 measures the field dependence of μ which depends on T and possibly on c, too, and f_1 measures the T-dependence of the zero-field mobility which may also depend on c. It is obvious from (25) that in order to determine the functional dependence of $\mu_0(c)$ one has to know the dependences of μ on both E and T, parametric in concentration. If $\mu(c)$ is

measured at constant T and E only, data analysis in terms of (25) or any other transport equation can only be a zero-order approach because it tacitly assumes f_1 and f_2 to be independent of c.

The homogeneous lattice model need not, however, be appropriate. Upon dilution a fraction of the sites otherwise available for transport are replaced by inert binder molecules. Intuitively, the model of choice for this problem appears to be the site percolation concept [81 to 83]. In the absence of disorder it predicts

$$\mu(c) \propto (c - c_0)^{\gamma} \tag{26}$$

with $c_0 = 0.312$ for a simple cubic structure and $\gamma = 1.5$ [82]. The percolation model takes proper account of the discrete molecular structure of the sample, yet is likely to overestimate the threshold behavior of $\mu(c)$ near the critical concentration since it ignores the possibility that a carrier leaves a dead end of a conducting path by a non-nearest neighbor jump permitted by virtue of the exponential distance dependence of the intersite jump rate. The critical behavior near c_0 is thus likely to be eroded.

In the absence of an analytic treatment of site percolation under the premise of exponential intersite coupling MC simulations were carried out yielding the charge carrier mobility in a diluted cubic system. To save computer time the computations were done on samples consisting of 70 lattice planes only and devoid of energetic disorder. The latter condition implies that the results be adequate for analysing experimental mobility data extrapolated to $T \to \infty$ where the effect of disorder has vanished. Fig. 34 presents MC data for $\mu(c)$ parametric in $2\gamma a$. They confirm the intuitive notion that erosion of criticality is the more pronounced the smaller $2\gamma a$ is, i.e. as the spatial extent of the wave function increases. Replotting the data on a $\ln(\mu c^{2/3})$ versus $c^{-1/3}$ scale reveals, however, that (24) does provide a reasonable approximation, at least for $c \gtrapprox 0.1$ (Fig. 35). This indicates that the homogeneous lattice model can, in fact, be considered as a zero-order approach to treat the concentration dependence of carrier motion in molecularly doped polymers. Plotting experimental $\mu(c)$ data in terms of (24) does at least yield the wave function overlap parameter $2\gamma a$ within an accuracy of about 20% [84].

To demonstrate the consistency between simulation and experimental results, the $\mu_0 c^{2/3}$-data Borsenberger [7] obtained for the system tritolylamine (TTA)/PC have been included in Fig. 35. They were obtained by plotting the zero-field mobilities on a $\ln \mu$ versus T^{-2} scale and extrapolating to $T \to \infty$ [7]. Data fitting by (24) yields $2\gamma a = 8.5$. Had one plotted the zero-field mobilities – extrapolated according to a $\ln \mu \propto E^{1/2}$ relationship – measured at room temperature one would have obtained $2\gamma a = 12.7$! The reason for the difference is that dilution causes the width of the DOS to increase as a result of the increasing randomness of the internal electric fields due to the randomly oriented dipoles of the polycarbonate binder. This causes the temperature effect on μ to increase the smaller c becomes.

At this stage it appears appropriate to outline and critically examine the small polaron approach Schein et al. [26] developed to analyse the concentration dependence of the hole mobility in the TTA/polycarbonate system. As mentioned in the Introduction the small polaron model rests on the ideal that the configuration of a hopping site is altered upon removal or addition of an extra electron. The charge is, therefore, dressed by a deformation it has to drag while moving. Polaron theory [85] predicts that the associated activation energy for transport is $\Delta = \frac{1}{2} E_p - J$ where E_p is the polaron binding energy and J the

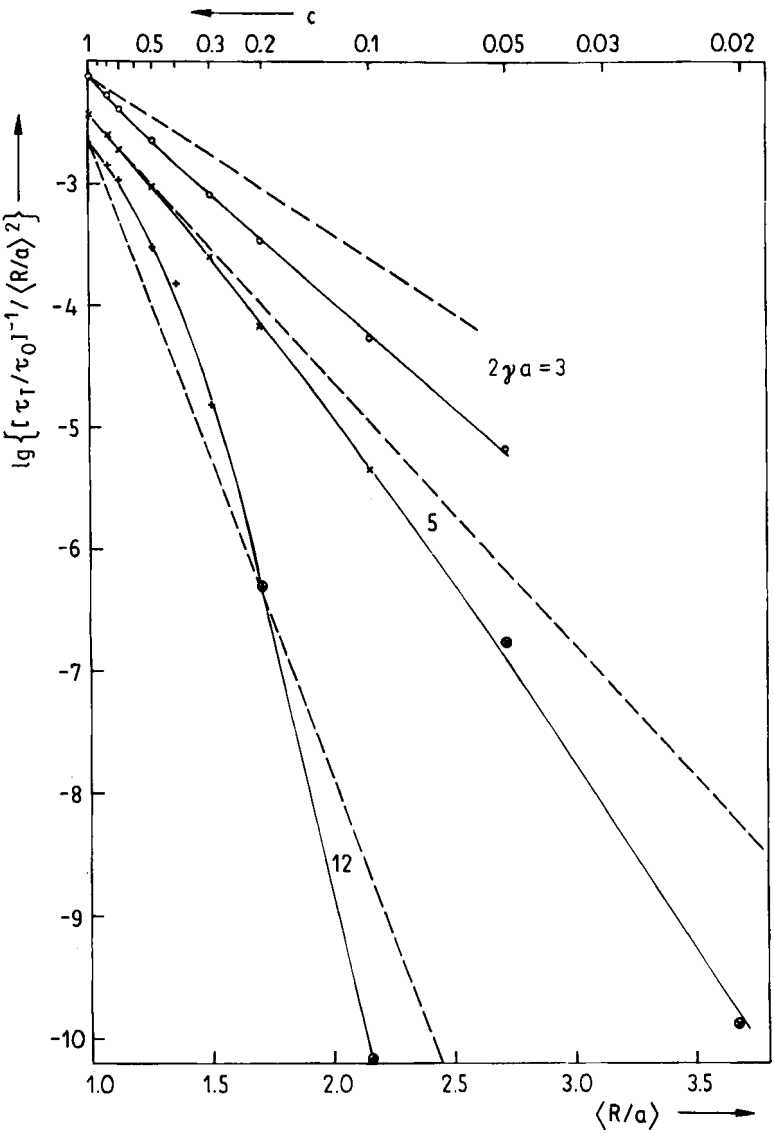

Fig. 34. Monte Carlo simulation results for the concentration dependence of the mobility plotted in accordance with the homogeneous lattice gas model (24) for various values of the wave function overlap parameter $2\gamma a$ (from [84]). τ_{tr} and τ_0 are identical with t_{tr} and t_0 used throughout this paper

charge transfer integral. The zero field mobility is

$$\mu(E = 0) = \frac{e}{kT} P c^{-2/3} \frac{\omega}{2\pi} \exp\left(-\frac{\Delta}{kT}\right), \tag{27}$$

P denoting the probability that a charge carrier will hop once an energy coincidence between donor and acceptor sites has been established via thermal activation. The adiabatic regime

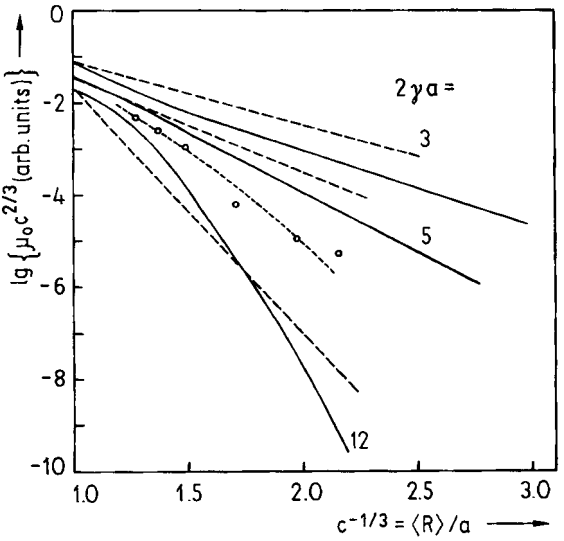

Fig. 35. Simulation data for $\mu(c)$ of Fig. 34 plotted on a lg $(\mu_0 c^{2/3})$ vs. $\langle R\rangle/a$ scale as suggested by the homogeneous lattice gas model. Dashed lines indicate 'theoretical' slopes (from [84]). Data points are experimental and were obtained by plotting the zero field mobilities of TTA/PC on a $\ln \mu$ vs. T^{-2} scale and extrapolating to $T \to \infty$ (from [9])

is defined as $P = 1$, i.e. charge transfer occurs with unit probability independent of site separation. Consequently, the product $\mu(E = 0)\, c^{2/3}$ should not depend on c as long as J is large. This condition cannot hold at large intersite distances because J decreases exponentially with increasing $\langle R\rangle$. In the non-adiabatic regime

$$P \propto J^2 \propto \exp\left(-(2\gamma a c^{-1/3})\right). \tag{28}$$

The transition from adiabatic to non-adiabatic small polaron transport should manifest itself in a break in the concentration dependence of $\mu_0(E = 0, T \to \infty)\, c^{2/3}$. At large c, this quantity should be constant and decrease exponentially with $c^{-1/3}$, i.e. increasing site distances, at low concentration.

Schein et al. [26] took experimental data for the hole mobility in TTA/lexane – the same systems Borsenberger had used for his study [7] – to verify their model. They plotted the zero-field mobilities, evaluated from $\ln \mu$ versus $E^{1/2}$ plots, in an Arrhenius diagram yielding $\mu(E = 0, T \to \infty)$. A plot of their $\mu(E = 0, T \to \infty)\, c^{2/3}$ data versus $\langle R\rangle/a = c^{-1/3}$ is shown in Fig. 36. A change from distance independent to distance dependent behavior, apparently verifying the polaron picture, is obvious. Note, however, that $T \to \infty$ mobilities saturate at $\approx 100\ \mathrm{cm^2/Vs}$ which is a prohibitively large value even for a molecular crystal. For comparison, Borsenberger's $\mu_0 c^{2/3}$ data, derived from the same raw data set but evaluated in terms of the hopping model, i.e. from a $\ln \mu$ versus T^{-2} plot (see Fig. 28), are neither anomalously larger nor do they bear out the transition from distance independence to distance dependence at a critical concentration. Note that the difference between the two plots is solely a consequence of the fact that extrapolation according to an Arrhenius plot overestimates $\mu(T \to \infty)$. This is a warning example how the choice of model affects the final result, and illustrates how hazardous $\mu(T)$ extrapolations over many decades are.

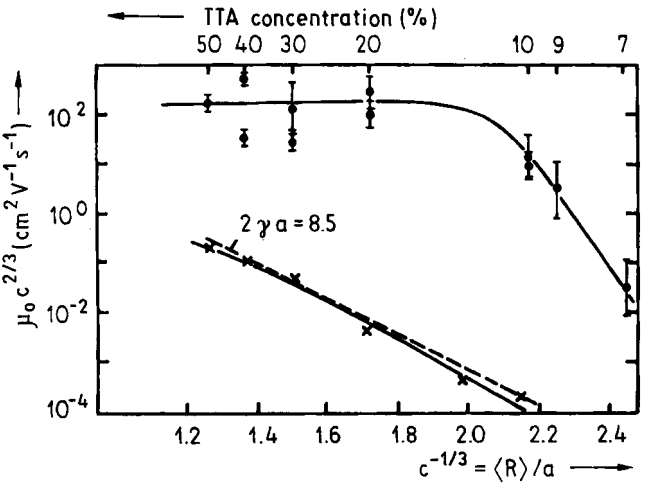

Fig. 36. Comparison of the $\mu_0 c^{2/3}$ data for TTA/PC obtained by extrapolating $\mu(T)$ according to Arrhenius' law (full symbols, taken from [26]) and according to a $\ln \mu$ vs. T^{-2} law, respectively (from Fig. 35 using data of Borsenberger et al. [9]). The dashed line is the prediction of the homogeneous lattice model for $2\gamma a = 8.5$

5. Guideline for Estimating Polaronic Effects

Despite the obvious success of the disorder concept for rationalizing charge transport in molecularly doped polymers — and, acording to recent work in π- [17, 97] and σ- [29] conjugated main chain polymers as well — it is legitimate to question the reason for this success and to outline problems that need to be addressed in future work. The main criticism the present approach has to face is the assumption of the Miller-Abrahams ansatz for the jump rate which, on the one hand, ignores polaronic effects but requires moderate electron phonon coupling on the other hand [86]. In a more realistic ansatz the prefactor in the jump rate had to carry a T-dependence. However, the strong T-dependence of μ certainly overrides any effect of a — presumably — power law dependence of ν_0 on T. As far as the consideration of a polaronic binding energy is concerned a simple estimate may provide a guideline for a crude assessment of its effect on $\mu(T)$.

A first approach to incorporate polaron effects is to invoke intramolecular relaxation of the charge carrying species upon oxidation or reduction. Let the average energy gain be E_p — any spread of E_p would be equivalent to increasing disorder — and show up in the expression for the jump rate by an extra Boltzmann factor carrying an activation energy $E_p/2$. Since all transition rates are affected in the same way the calculation can be done in factorized form and the total, albeit temperature dependent, activation energy of transport would then be the sum of a disorder and a polaron contribution (see (10)),

$$\Delta = \Delta^{\mathrm{pol}} + \Delta^{\mathrm{dis}} = \frac{E_p}{2} + \frac{8}{9}\sigma\hat{\sigma}\,. \tag{29}$$

Considering the inherent difficulty to distinguish $\ln \mu$ versus T^{-1} and T^{-2} plots covering a small T-range only, any deviation from a $\ln \mu$ versus T^{-2} plot would hardly be discernible.

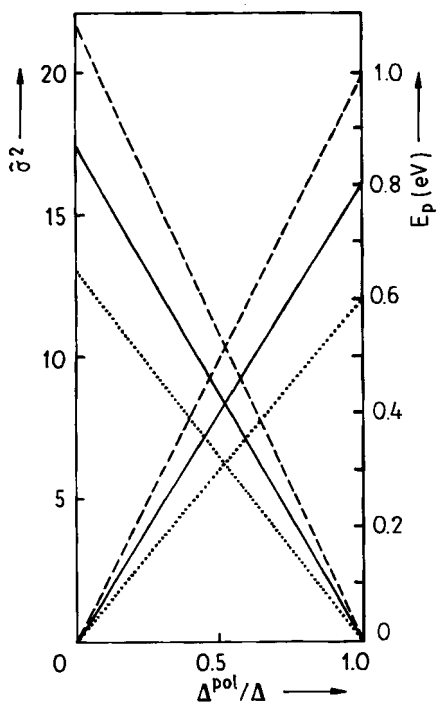

Fig. 37. Estimate of $\hat{\sigma}^2$ (left scale) and of the polaron binding energy E_p (right scale) for variable relative polaron contribution to the measured total "activation energy" Δ of the mobility for $\Delta = 0.5$ (– – –), 0.4 (———), 0.3 eV (· · · · · · ·)

A critical test for a polaronic or any other simply activated contribution to T-dependent transport such as shallow trapping is, however, provided by the comparison between the temperature dependence of the carrier mobility and the onset of dispersion of TOF signals at lower temperatures. If both sets of data are consistent, as is the case for DEH (see Section 4.5), the polaronic contribution must be negligible as compared with disorder effects. If, on the other hand, onset of dispersion starts at lower temperature, i.e. smaller $\hat{\sigma}$, this provides a handle on separating disorder from polaron effects. Since only half of E_p contributes to Δ while – because of the offset of the occupational DOS from the real DOS by σ^2/kT (see Section 4.1) – the disorder contribution is a multiple of σ, a quite moderate polaronic contribution to Δ can translate into a quite large ratio of E_p/σ. This is illustrated in Fig. 37 showing both $\hat{\sigma}^2$ and E_p as a function of the fractional polaron contribution Δ^{pol}/Δ for $\Delta = 0.5$, 0.4, and 0.3 eV, respectively, while Fig. 38 presents E_p/σ versus Δ^{pol}/Δ. If, for instance, the σ-values

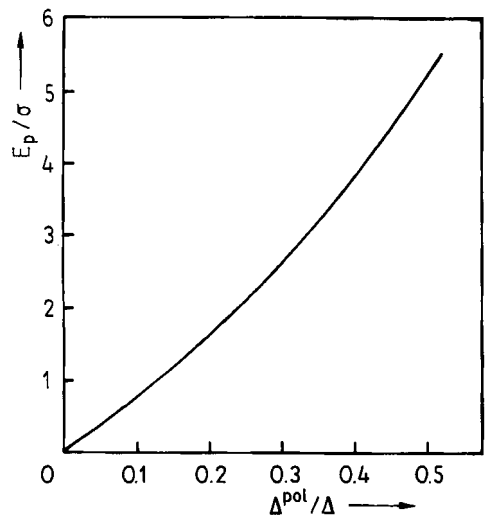

Fig. 38. E_p/σ vs. Δ^{pol}/Δ

calculated from $\mu(T)$-data, on the one hand, and from the temporal evolution of TOF signals, on the other hand, agreed to within 4% (equivalent to ≈ 10 K uncertainty concerning the onset temperature of dispersion) any polaronic contribution to Δ may be $\leqq 8\%$ equivalent to $E_p/\sigma = 0.5$. Since σ is typically around 0.1 eV this implies that a 50 meV polaronic binding energy is below the limit an analysis of transport data would allow to separate. The message of this order of magnitude estimate is that small polaronic contributions to Δ, which must occur because the equilibrium configurations of a neutral transport molecule and a radical cation/anion are inevitably different and which have been invoked for rationalizing charge transport in crystals [43], are compatible with data analysis in terms of the disorder formalism. In how far larger contributions would modify the expected field dependence of μ remains to be explored in future work. Suffice to mention here that pure polaronic transport should yield a $\mu(E) \propto E^{-1} \sinh(eEa/2kT)$ relation that has never been observed in experiment.

6. Concluding Remarks

The present review summarizes how hopping motion of charge carriers in a Gaussian density of localized states with or without superimposed off-diagonal disorder is revealed in experimental observables such as the dependence of the carrier mobility on temperature, electric field, composition in the case of multicomponent systems, and TOF profiles. It has been shown that the recurrent features observed with chemically very different systems can be understood in terms of a model that is conceptionally simple, yet extremely difficult to tackle analytically. Monte Carlo simulations are, however, a convenient tool to determine how the combination of physical assumptions, for instance, the form of the intersite jump rate, and material parameters such as the degree of diagonal and off-diagonal disorder translate into macroscopic properties.

In terms of the disorder model the similar behavior of a variety of polymeric photoconductors is a consequence of the similar degree of disorder they contain. This, in turn, is a natural consequence of similar preparation conditions. They are usually solution cast by letting the solvent evaporate at room temperature. Therefore, the energetic distribution of metastable conformation trapped within the structure should not be too different. It translates into DOSs typically 0.1 eV wide equivalent to an activation energy of the mobility of ≈ 0.4 eV if inferred from the tangent to an Arrhenius plot at 300 K. It is also manifest in the similar inhomogeneous broadening of optical absorption spectra, their common origin being random internal fields in random matrices that act on both a dipole, such as an exciton, or a charge located on a transport molecule [87]. Qualitative support for this reasoning comes from the matrix dependence of μ that translates into a matrix dependence of the width of the DOS [88] and, notably, a dependence of σ on the presence of dipolar additives [89] and on the dipole moments of either the transport [10, 90] or host molecules [88] or both [91]. Quantifying such empirical relations by calculating the distribution of internal fields and, concomitantly, width and profile of the DOS, is a challenge for future work. An experimental starting point may be the evaluation of the random internal fields on the basis of Stark effect measurements employing hole burning spectroscopy of chromophons embedded in random matrices [92 to 94]. The recent work of Novikov and Vannikov [95] on the effect of dipolar traps on the field dependence of μ offers a complementary approach.

Acknowledgements

I am highly indebted to L. Pautmeier, R. Richert, and B. Ries for their contribution to this work. Stimulating discussions and the exchange of ideas and information with M. Abkowitz, P. Borsenberger, B. Movaghar, L. Schein, M. Silver, M. Stolka, and R. Young are gratefully acknowledged, as is the generous support by the Deutsche Forschungsgemeinschaft and the Fonds der Chemischen Industrie. The collaboration with M. Silver was supported by a NATO travel grant.

References

[1] M. A. ABKOWITZ, M. STOLKA, and M. MORGAN, J. appl. Phys. **52**, 3453 (1981).
[2] H. BÄSSLER, G. SCHÖNHERR, M. A. ABKOWITZ, and D. M. PAI, Phys. Rev. B **26**, 3105 (1982).
[3] M. STOLKA, J. F. YANUS, and D. M. PAI, J. phys. Chem. **88**, 4707 (1984).
[4] S. J. SANTOS LEMUS and J. HIRSCH, Phil. Mag. **B53**, 25 (1986).
[5] L. B. SCHEIN, A. ROSENBERG, and S. L. RICE, J. appl. Phys. **60**, 4287 (1986).
[6] A. PELED, L. B. SCHEIN, and D. GLATZ, Phys. Rev. B **41**, 10835 (1990).
[7] P. M. BORSENBERGER, J. appl. Phys. **68**, 6263 (1990).
[8] H. J. YUH and D. M. PAI, Phil. Mag. Letters **62**, 61 (1990).
[9] P. M. BORSENBERGER, T. M. KUNG, and W. B. VREELAND, J. appl. Phys. **68**, 4100 (1990).
[10] M. SUGIUCHI, H. NISHIZAWA, and T. UEHARA, Proc. 6th Internat. Congr. Advances in Nonimpact Printing Technologies, Ed. R. J. NASH, The Society for Imaging Science and Technology, Springfield (VA) 1990 (p. 298).
[11] T. KITAMURA and M. YOKOYAMA, J. appl. Phys. **69**, 821 (1991).
[12] Y. KANEMITSU, H. FUNADA, and Y. MATSUMOTO, J. appl. Phys. **71**, 300 (1992).
[13] R. G. KEPLER, J. M. ZEIGLER, L. A. HARRAH, and S. R. KURTZ, Phys. Rev. B **35**, 2818 (1987).
[14] M. A. ABKOWITZ and M. STOLKA, Phil. Mag. Letters **58**, 239 (1988).
[15] M. A. ABKOWITZ, M. J. RICE, and M. STOLKA, Phil. Mag. **B61**, 25 (1990).
[16] T. TAKIGUCHI, D. H. PARK, H. UENO, K. YOSHINO, and R. SUGIMOTO, Synth. Metals **17**, 1111 (1987).
[17] M. GAILBERGER and H. BÄSSLER, Phys. Rev. B **44**, 8643 (1991).
[18] P. STROHRIEGL and D. HAARER, Makromol. Chem., Macromol. Symp. **44**, 85 (1991).
[19] F. C. BOS and D. M. BURLAND, Phys. Rev. Letters **58**, 152 (1987).
[20] E. MÜLLER-HORSCHE, D. HAARER, and H. SCHER, Phys. Rev. B **35**, 1273 (1987).
[21] H. SCHER and E. W. MONTROLL, Phys. Rev. B **12**, 2455 (1975).
[22] G. PFISTER, Phys. Rev. B **16**, 3676 (1977).
[23] G. PFISTER and H. SCHER, Adv. Phys. **27**, 747 (1978).
[24] G. GIRO and P. G. DIMARCO, Chem. Phys. Letters **162**, 221 (1989).
[25] D. M. PAI, J. F. YANUS, M. STOLKA, D. RENFER, and W. W. LIMBURG, Phil. Mag. **B48**, 505 (1983).
[26] L. B. SCHEIN, D. GLATZ, and J. C. SCOTT, Phys. Rev. Letters **65**, 472 (1990).
[27] A. PELED and L. B. SCHEIN, Chem. Phys. **153**, 422 (1988).
[28] K. YOKOYAMA and M. YOKOYAMA, Phil. Mag. **B61**, 59 (1990).
[29] M. A. ABKOWITZ, H. BÄSSLER, and M. STOLKA, Phil. Mag. **B63**, 201 (1991).
[30] P. M. BORSENBERGER, L. PAUTMEIER, and H. BÄSSLER, J. phys. Chem. **94**, 5447 (1991).
[31] H.-J. YUH and M. STOLKA, Phil. Mag. **B58**, 539 (1988).
[32] E. A. SILINSH, Organic Molecular Crystals, Their Electronic States, Springer Ser. Solid State Phys., Vol. 16, Springer-Verlag, Berlin 1980.
[33] H. BÄSSLER, phys. stat. sol. (b) **107**, 9 (1981).
[34] M. R. V. SAHYUN, Photogr. Sci. Engng. **28**, 185 (1984).
[35] L. B. SCHEIN and J. X. MACK, Chem. Phys. Letters **149**, 109 (1988).
[36] A. V. VANNIKOV, A. YU. KRYUKOV, A. G. TURIN, and T. S. ZHURAVLEVA, phys. stat. phys. (a) **115**, K47 (1989).
[37] C. VERBEEK, M. VAN DER AUWEAER, F. C. DESCHRYVER, C. GEELEN, D. TERRELL, and S. DEMENTER, Chem. Phys. Letters **188**, 85 (1992).
[38] N. SATO, H. INOKUCHI, and E. A. SILINSH, Chem. Phys. **115**, 269 (1987).

[39] H. BÄSSLER, Makromol. Chem., Macromol. Symp. **37**, 1 (1990).
[40] R. JANKOWIAK, K. D. ROCKWITZ, and H. BÄSSLER, J. phys. Chem. **87**, 552 (1983).
[41] R. F. MAHRT, J. YANG, and H. BÄSSLER, Chem. Phys. Letters **192**, 576 (1992).
[42] V. M. KENKRE, J. D. ANDERSEN, D. H. DUNLAP, and C. B. DUKE, Phys. Rev. Letters **62**, 1165 (1989).
[43] A. MILLER and E. ABRAHAMS, Phys. Rev. **120**, 745 (1960).
[44] J. H. SLOWIK and I. CHEN, J. appl. Phys. **54**, 4467 (1983).
[45] B. MOVAGHAR, M. GRÜNEWALD, B. RIES, H. BÄSSLER, and D. WÜRTZ, Phys. Rev. B **33**, 5545 (1986).
[46] B. RIES, H. BÄSSLER, M. GRÜNEWALD, and B. MOVAGHAR, Phys. Rev. B **37**, 5508 (1988).
[47] A. BLUMEN, J. KLAFTER, B. S. WHITE, and G. ZUMOFEN, Phys. Rev. Letters **53**, 1301 (1989).
[48] G. KÖHLER and A. BLUMEN, J. Phys. A **20**, 5627 (1987).
[49] D. HAARER, H. SCHNÖRER, and A. BLUMEN, in: Dynamical Processes in Condensed Molecular Systems, Ed. J. KLAFTER, J. JORTNER, and A. BLUMEN, World Scientific Publ. Co., Singapore 1989 (p. 107).
[50] G. SCHÖNHERR, H. BÄSSLER, and M. SILVER, Phil. Mag. **B44**, 47 (1981).
[51] N. F. MOTT and E. A. DAVIS, Electronic Processes in Non-Crystalline Materials, 2nd ed., Clarendon Press, Oxford 1978.
[52] L. PAUTMEIER, R. RICHERT, and H. BÄSSLER, Phil. Mag. Letters **59**, 325 (1989).
[53] B. MOVAGHAR, B. RIES, and M. GRÜNEWALD, Phys. Rev. B **34**, 5574 (1986).
[54] R. RICHERT and H. BÄSSLER, J. chem. Phys. **84**, 3567 (1986).
[55] R. RICHERT, H. BÄSSLER, B. RIES, B. MOVAGHAR, and M. GRÜNEWALD, Phil. Mag. Letters **59**, 95 (1989).
[56] D. L. HUBER, J. chem. Phys. **78**, 2530 (1983).
[57] U. LARSEN, Phys. Rev. B **32**, 1772 (1985).
[58] U. LARSEN, Phys. Letters A **105**, 307 (1984).
[59] J. D. FERRY, L. D. GROMDINE, and E. R. FITZGERALD, J. appl. Phys. **24**, 912 (1953).
[60] P. M. BORSENBERGER, L. PAUTMEIER, R. RICHERT, and H. BÄSSLER, J. chem. Phys. **94**, 8276 (1991).
[61] L. PAUTMEIER, R. RICHERT, and H. BÄSSLER, Synth. Metals **37**, 271 (1990).
[62] H. BÄSSLER, Phil. Mag. **B50**, 347 (1984).
[63] B. MOVAGHAR, A. YELON, and M. MEUNIER, Chem. Phys. **146**, 389 (1990).
[64] L. PAUTMEIER, R. RICHERT, and H. BÄSSLER, Phil. Mag. **B63**, 587 (1991).
[65] L. PAUTMEIER, B. RIES, R. RICHERT, and H. BÄSSLER, Chem. Phys. Letters **143**, 459 (1988).
[66] H. BÖTTGER and V. V. BRYKSIN, phys. stat. sol. (b) **96**, 219 (1979).
[67] N. VAN LIEN and B. I. SHKLOVSKII, Solid State Commun. **38**, 99 (1981).
[68] E. I. LEVIN and B. I. SHKLOVSKII, Solid State Commun. **67**, 233 (1988).
[69] W. G. GILL, J. appl. Phys. **43**, 5033 (1972).
[70] H. SCHER, M. F. SCHLESINGER, and J. T. BENDLER, Phys. today **43**, 26 (1990).
[71] L. B. SCHEIN, J. C. SCOTT, L. T. PAUTMEIER, and R. H. YOUNG, Mol. Cryst. liquid Cryst., in the press.
[72] R. H. YOUNG, private communication.
[73] P. M. BORSENBERGER, private communication.
[74] A. I. RUDENKO and V. I. ARKHIPOV, Phil. Mag. **B45**, 177 (1982).
[75] J. B. BOUCHAUD and A. GEORGES, C.R. Acad. Sci. (France), Ser II, 1431 (1988); Phys. Rev. Letters **63**, 2692 (1989).
[76] P. M. BORSENBERGER, L. PAUTMEIER, and H. BÄSSLER, Phys. Rev. B, in press.
[77] P. M. BORSENBERGER, R. RICHERT, and H. BÄSSLER, submitted to Phys. Rev. B.
[78] G. PFISTER and C. H. GRIFFITH, Phys. Rev. Letters **40**, 659 (1978).
[79] D. M. PAI, J. F. YANUS, and M. STOLKA, J. phys. Chem. **88**, 4714 (1984).
[80] J. HIRSCH, J. Phys. C **12**, 321 (1979).
[81] M. SILVER, K. RISKO, and H. BÄSSLER, Phil. Mag. **B40**, 247 (1979).
[82] S. KIRKPATRICK, Rev. mod. Phys. **45**, 576 (1973).
[83] D. STAUFFER, Physics Rep. **54**, 1 (1979).
[84] B. RIES, H. BÄSSLER, and M. SILVER, Phil. Mag. **B54**, 141 (1986).
[85] D. EMIN, in: Electronic and Structural Properties of Amorphous Semiconductors, Chap. 7, Ed. P. G. LECOMBER and J. MORT, Academic Press, New York 1973.
[86] L. B. SCHEIN, Phil. Mag. **B65**, 795 (1992).

[87] A. ELSCHNER, R. F. MAHRT, L. PAUTMEIER, H. BÄSSLER, M. STOLKA, and K. M. MCGRANE, Chem. Phys. **150**, 81 (1991).
[88] P. M. BORSENBERGER and H. BÄSSLER, J. chem. Phys. **95**, 5327 (1991).
[89] P. M. BORSENBERGER and H. BÄSSLER, phys. stat. sol. (b) **170**, 291 (1992).
[90] P. M. BORSENBERGER, Proc. ERPOS VI Conf., Capri 1992; Mol. Cryst. liquid Cryst., to be published.
[91] P. M. BORSENBERGER, private communication.
[92] A. J. MEIXNER, A. RENN, and U. P. WILD, Chem. Phys. Letters **190**, 75 (1992).
[93] M. MAREN, Appl. Phys. B **41**, 43 (1986).
[94] L. KADOR, D. HAARER, and P. I. PERSONOV, J. chem. Phys. **86**, 5300 (1987).
[95] S. V. NOVIKOV and A. V. VANNIKOV, Chem. Phys. Letters **182**, 598 (1991).
[96] P. M. BORSENBERGER and H. BÄSSLER, J. Imag. Sci. **35**, 79 (1991).
[97] N. T. BINH, L. Q. MINH, and H. BÄSSLER, Synth. Metals, in the press.
[98] J. C. SCOTT, L. TH. PAUTWEIN, and L. B. SCHEIN, Phys. Rev. B, in the press.

(Received September 11, 1992)